A Head Up Display for Application to V/STOL Aircraft Approach and Landing

Vernon K. Merrick, Glenn G. Farris, and
Andrejs A. Vanags

NASA

NASA Technical Memorandum 102216

A Head Up Display for Application to V/STOL Aircraft Approach and Landing

Vernon K. Merrick and Glenn G. Farris, Ames Research Center, Moffett Field, California
Andrejs A. Vanags, SYRE Corporation, Moffett Field, California

January 1990

NASA

National Aeronautics and
Space Administration

Ames Research Center
Moffett Field, California 94035

TABLE OF CONTENTS

NOMENCLATURE

The display contains a large number of independent pieces of information derived from the extensive processing of a large number of aircraft sensor signals. The result is that a large nomenclature is required to present a detailed analytical description of the display format. To create a degree of order, some rules have been adopted in the assigning of mathematical symbols to the various quantities. These rules are given below.

- With the exception of the display coordinates, (X, Y), all variables are designated by lower case symbols (Roman or Greek).
- With the exception of the acceleration due to gravity, g, all constants are designated by upper case symbols (Roman or Greek). Mode identifiers are regarded as constants.
- Each gain or scale factor is designated by a subscripted k, if a variable, or a subscripted K, if a constant.
- Each time constant is designated by a subscripted T.
- Each mode identifier is designated by a subscripted I.
- All display symbol positions are designated by subscripted coordinates (X, Y).

The nomenclature is divided into the following four categories:

1. Continuous and discrete input variables. The continuous input variables are obtained from the aircraft's sensors, and the discrete variables are operating-mode alternatives.
2. Intermediate variables used in the description of the display-symbol drive laws
3. Constants
4. Output variables in the form of display coordinates

Input Variables

Continuous

a_{yp}	aircraft body-axis lateral acceleration at the cockpit, ft/sec^2
h	true altitude of the aircraft's center of gravity, (c.g.), ft
$\dot{h}$	vertical velocity of the aircraft's c.g., ft/sec
$\ddot{h}$	vertical acceleration of the aircraft's c.g., ft/sec^2
h_t	height of the aircraft's c.g. above the reference touchdown point, ft
$\dot{h}_c$	pilot-commanded vertical velocity of the aircraft's c.g., ft/sec
$\dot{h}_l$	vertical velocity of the desired touchdown point, ft/sec
v_n, v_e	north and east velocities of the aircraft's c.g. relative to the station-keeping point, ft/sec
$\dot{v}_n, \dot{v}_e$	north and east accelerations of the aircraft's c.g., ft/sec^2
v_a	airspeed, ft/sec
v_{xc}, v_{yc}	pilot-commanded longitudinal and lateral velocities of the aircraft's c.g. relative to the station-keeping point, ft/sec
$\dot{v}_{xc}$	pilot-commanded longitudinal acceleration of the aircraft's c.g., ft/sec^2
x, y, z	general coordinates in a north-east-down axis system whose origin is at the landing pad datum, ft

x_a, y_a	horizontal coordinates of the aircraft's c.g. in the (x, y, z) axis system, ft
α	angle of attack, deg
δ_t	throttle position, deg
δ_x	longitudinal control input, in.
δ_y	lateral control input, in.
ϕ, θ, ψ	aircraft roll, pitch, and yaw Euler angles, deg
$\dot{\phi}, \dot{\theta}, \dot{\psi}$	aircraft roll, pitch, and yaw Euler-angle rates, deg/sec
θ_j	engine nozzle angle, deg
$\dot{\theta}_j$	engine nozzle angular rate, deg/sec
ψ_{wod}	heading of the mean wind over the landing pad, deg

Discrete

I_a	longitudinal translational command mode in the approach
I_{at}	type of attitude control mode
I_d	heave damper select
I_l	type of landing (conventional or vertical)
I_v	horizontal translational command mode in hover
I_w	vertical command mode

Intermediate Variables

d	distance of the aircraft's c.g. from the station-keeping point, measured along the reference flightpath track, ft
d_i	range at the start of deceleration, ft
d_p^j	horizontal distance of the jth landing-pad vertex from the pilot's eyepoint, ft
f_a	position of the longitudinal acceleration caret relative to the flightpath symbol, deg
f_{ae}	length of the longitudinal acceleration error ribbon, deg
f_u	length of the longitudinal velocity error line, deg
f_{ay}	displacement of the lateral acceleration ball from the center of the flightpath symbol, deg
f_s	distance of the longitudinal position indicator from the flightpath symbol, deg
$\widehat{\ddot{h}}$	filtered estimate of the vertical acceleration, ft/sec^2
$\widehat{\dot{h}}_c$	estimated commanded vertical velocity, ft/sec
h_g	height of the ghost aircraft datum (vertex a), ft
h_r	altitude of the reference flightpath at the position of the aircraft's c.g., ft
i	indicates whether the local reference flightpath is straight ($i = 0$) or curved, and, if curved, whether to the right ($i = +1$) or to the left ($i = -1$)
k_{wg}	ghost lead blending gain
k_θ	pitch rate blending gain
k_ϕ	turn entry-and-exit blending gain
k_{δ_t}	throttle washout gain, ft/deg sec

$l^{(i)}$	length of the line from the aircraft to the appropriate reference flightpath circle, ft
s	Laplace transform variable, 1/sec
t_{bx}, t_{by}	coordinates of the velocity predictor ball relative to the trident symbol, deg
t_{lx}, t_{ly}	coordinates of the datum of the landing-pad symbol relative to the trident symbol, deg
t_{lh}	position of the landing-pad bar relative to the trident symbol, deg
t_{sx}, t_{sy}	coordinates of the station-keeping point cross relative to the trident symbol, deg
t_{vx}, t_{vy}	coordinates of the moving tip of the velocity vector relative to the trident symbol, deg
t_{wc}	position of the vertical velocity predictor diamond relative to the trident symbol, deg
t_{wl}	length of the vertical velocity limit ribbon, deg
$\widehat{v}_a$	estimated acceleration relative to the airmass, ft/sec^2
v_{af}	filtered airspeed, ft/sec
v_{rt}	aircraft speed along the reference flightpath, ft/sec
$\dot{v}_r$	reference longitudinal acceleration along the reference flightpath track, ft/sec^2
$\dot{v}_{rt}$	acceleration along the reference flightpath, ft/sec^2
$\widehat{\dot{v}}_{rt}$	filtered acceleration along the reference flightpath, ft/sec^2
v_x, v_y	horizontal longitudinal and lateral velocities relative to the station-keeping point, ft/sec
v_{tl}	limited horizontal velocity relative to the station-keeping point, ft/sec
$\dot{v}_x, \dot{v}_y$	longitudinal and lateral accelerations relative to the station-keeping point, ft/sec^2
$\widehat{\dot{v}}_x, \widehat{\dot{v}}_y$	filtered longitudinal and lateral accelerations relative to the station-keeping point, ft/sec^2
x', y'	general coordinates in an axis system whose origin is at the center of the appropriate reference flightpath circle and whose x axis is parallel to the final flightpath segment, ft
x'_a, y'_a	coordinates of the aircraft's c.g. in the (x', y') axis system, ft
x'', y'', z''	general coordinates in an axis system whose origin is at the landing-pad datum, and which is generated by rotating the standard north-east-down axis system about the vertical axis, through the aircraft's heading angle, ft
x''_p, y''_p, z''_p	coordinates of the pilot's eyepoint in the (x'', y'', z'') axis system, ft
$\widehat{\alpha}$	filtered angle of attack, deg
$\widehat{\beta}$	angle of the mean wind relative to the aircraft's longitudinal axis, deg
γ	inertial flightpath angle, deg
γ_p	potential flightpath angle, deg
γ_q	quickened flightpath angle, deg
$\delta x''^j$	x coordinate of jth landing-pad vertex, in the (x'', y'', z'') axis system, ft
$\delta y''^j$	y coordinate of jth landing-pad vertex, in the (x'', y'', z'') axis system, ft

$\delta z''^j$	z coordinate of jth landing-pad vertex, in the (x'', y'', z'') axis system, ft
$\delta x_{gv}, \delta x_{gh}$	distances of the ghost aircraft ahead of the real aircraft for the lateral and vertical tracking tasks, ft
δy	lateral distance of the aircraft from the reference flightpath track, ft
$\delta\eta'_{g-}, \delta\mu'_{g-}$ $(- = b, c,$ $d, e, f, g)$	elevation and azimuth of the defining vertices b, c, d, e, f, g of the ghost aircraft relative to the ghost beacon (vertex a), deg
δ_{μ_g}	correction to the ghost aircraft lateral position to provide turn coordination at turn entry and exit, deg
ϵ	lateral inertial flightpath angle, deg
ϵ_q	quickened lateral flightpath angle, deg
θ_c, ϕ_c	pilot-commanded pitch and roll angles, deg
η_g, μ_g	elevation and azimuth angles of the ghost aircraft relative to the pilot's eyepoint, deg
η'_g, μ'_g	elevation and azimuth deviations of the ghost aircraft due to aircraft position errors relative to the reference flightpath, deg
η^j_p, μ^j_p	elevation and azimuth of the jth landing-pad (or runway) vertex, deg
λ	angle between a line from the aircraft to the center of the reference flightpath circle and the x axis of the landing pad, deg
ν	angle subtended at the center of the reference flightpath circle by the remaining arc of the circular flightpath segment, deg
$\sigma_u, \sigma_v, \sigma_w$	longitudinal, lateral, and heave damping parameters, 1/sec
ψ_l	heading of the x axis of the landing pad, deg
ψ_{la}	heading of the x axis of the landing pad relative to the aircraft's longitudinal axis, deg
ψ_{pa}	heading of the landing-pad pointer relative to the aircraft's longitudinal axis, deg
ψ_t	heading of the tangent to the reference flightpath track, deg

Constants

A	approach maximum angle of attack, deg
$A_{\delta t}$	change of gross thrust per unit of aircraft mass per unit change of throttle position, ft/deg sec^2
B_x, B_y	coordinates of the start of the curved segment of the trajectory, expressed in the mean landing-pad axis system, ft
C_x, C_y	coordinates of the start of the final straight segment of the flightpath, in the mean landing-pad axis system, ft
D_b, D_c	ranges at the curved flightpath entry and exit, ft
D_f	nominal range at the start of the second-step deceleration, ft
D_h	range at which the aircraft would come to a hover if the nominal first-step deceleration were held constant, ft
g	acceleration due to gravity (32.2 ft/sec^2)
H	reference hover altitude, ft

$\dot{H}$ — recommended maximum touchdown vertical velocity relative to the landing pad, ft/sec

K_{ax}, K_{ay} — scale factors converting linear accelerations to display angles, deg sec^2/ft

K_l, K_{la} — scale factors converting horizontal distances to display angles, deg/ft

K_h — scale factor converting vertical distances to display angles, deg/ft

K_u, K_{ua} — scale factors converting horizontal velocities to display angles, deg sec/ft

K_w — scale factor converting vertical velocities to display angles, deg sec/ft

$K_{\delta_x}, K_{\delta_y}$ — longitudinal and lateral control input gains used in calculations of estimated longitudinal and lateral accelerations in hover ($I_{at} = 0$), ft/in. sec

K_{δ_t} — maximum value of $k_{\delta t}$, ft/deg sec

K_ϵ — lateral flightpath angle scale factor

K_{θ_c}, K_{ϕ_c} — longitudinal and lateral control input gains used in calculations of estimated longitudinal and lateral accelerations in hover ($I_{at} = 1$), ft/deg sec

K_θ — vertical flightpath response gain, ft/deg sec

K_{ϕ_g} — ghost aircraft turn coordination washout gain

K_ϕ — lateral flightpath response gain, ft/deg sec

L_g — nominal distance of the wheels below the aicraft's c.g., ft

R — radius of curvature of the reference flightpath track, ft

R_p — radius of the circle on which the landing-pad pointer moves, deg

$R_x^{(i)}, R_y^{(i)}$ — coordinates of the centers of the reference flightpath circles in the mean landing-pad axis system, ft

S_x, S_y — coordinates of the station-keeping point in the mean landing-pad axis system, ft

T_1 — time constant of the airspeed and angle-of-attack filters, sec

T_2 — pitch and roll stick-input washout time constant, sec

T_4 — complementary filter time constant used in the calculation of filtered acceleration relative to the air mass, sec

T_5 — filter time constant used in the calculation of filtered inertial acceleration along the track, sec

T_6 — complementary time constant used in the calculation of filtered longitudinal and lateral accelerations in hover, sec

T_h — time constant of the desired vertical velocity response, sec

T_u — time constant of the desired airspeed response, sec

$T_{\dot{v}}$ — horizontal tracking time constant, sec

T_{ϕ_g} — ghost aircraft turn coordination washout time constant, sec

V_a — reference airspeed, ft/sec

$\dot{V}_f$ — nominal final deceleration, ft/sec^2

$\dot{V}_i$ — nominal initial deceleration, ft/sec^2

V_{vl} — inertial longitudinal speed below which the velocity error line is displayed when $I_l = 1$, ft/sec

$V_{f_{min}}$ — preset minimum value of the filtered airspeed used in the calculation of the pitch rate gain, k_θ, ft/sec

$V_{f_{max}}$	preset maximum value of the filtered airspeed used in the calculation of the pitch rate gain, $k_{\dot{\theta}}$, ft/sec
$V_{t_{min}}$	preset minimum value of v_{xl}, ft/sec
X_{max}	maximum value of the X display coordinates, deg
Y_{max}, Y_{min}	maximum and minimum values of the Y display coordinates, deg
Γ	reference vertical flightpath angle, deg
ΔT_f	time period of the final deceleration, sec
$\Delta T_{gh}, \Delta T_{gv}$	ghost lead times for the vertical and lateral tracking tasks, sec
$\Delta x^j, \Delta y^j$ Δz^j	x, y, z coordinates of the jth landing-pad vertex in a landing-pad fixed-axis system, ft
$\Delta D_b, \Delta D_c$	lead blend distances at the curved flightpath entry and exit, ft
$\Delta \eta, \Delta \mu, \Delta \chi$	fin height, semispan, and length of the ghost aircraft, deg
$\Delta \Psi_f$	heading of the final flightpath segment relative to the mean x axis of the landing pad, deg
$\Delta \Psi_l$	angle between a line from the aircraft to the center of the reference flightpath circle and the mean x axis of the landing pad, deg
$\Delta \Psi_i$	heading of the final flightpath segment relative to the mean x axis of the landing pad, deg
Θ	nominal pitch angle for the approach and landing, deg
$\Sigma_u, \Sigma_v, \Sigma_w$	estimates of the aircraft's longitudinal, lateral, and heave damping parameters in hover, 1/sec
$\Sigma_u', \Sigma_v', \Sigma_w'$	estimates of the average rate of change of the longitudinal, lateral, and heave damping parameters with airspeed over the normal approach airspeed range, 1/ft
Σ_{wc}	damping constant of the vertical velocity command mode, 1/sec
Σ_{wd}	heave damper constant, 1/sec
N_0	angle subtended at the center of the reference flightpath circle by the complete arc of the flightpath's circular segment, deg
Ψ	mean heading of the x axis of the landing pad, deg
Ψ_f	heading of the final segment of the reference flightpath, deg
Ψ_i	heading of the initial segment of the reference flightpath, deg

Output Variables (Display Coordinates)

The position of each symbol on the display is identified by coordinates (X, Y), subscripted and superscripted to identify the particular symbol.

Subscripts

a	longitudinal acceleration caret
ae	longitudinal acceleration error ribbon
ay	lateral acceleration ball
b	horizontal velocity predictor ball
f	flightpath symbol (limited)
fu	flightpath symbol (unlimited)
g	fin beacon (vertex a) of the ghost aircraft symbol (limited)

gu	fin beacon of the ghost aircraft symbol (unlimited)
$g-$ ($-=b,$	ghost aircraft vertices b, c, d, e, f, g
c, d, e, f, g)	
h	center of the horizon
l	datum of the landing-pad symbol (plan view)
lh	landing-pad bar
p	conformal landing-pad symbol
s	longitudinal position indicator
sc	station-keeping point cross
sp	station-keeping point pointer
t	trident symbol
v	horizontal velocity vector
ux	velocity error line
w	vertical velocity predictor diamond
wl	vertical velocity limit ribbon
αm	angle-of-attack warning bar
αr	angle-of-attack reference brackets

Superscripts

j	jth vertex of the landing pad

Variables without Subscripts or Superscripts

The list of output quantities needed to drive the HUD symbols is completed by those which define angular positions.

$\delta\phi_g$	angle of the ghost aircraft wings relative to the display abscissa (real aircraft wings), deg
ϕ	angle of the horizon bar relative to the display abscissa, deg
ϕ_g	angle of the ghost wings relative to the horizon bar, deg

A HEAD UP DISPLAY FORMAT FOR APPLICATION TO V/STOL AIRCRAFT APPROACH AND LANDING

Vernon K. Merrick, Glenn G. Farris, and Andrejs A. Vanags*

Ames Research Center

SUMMARY

This paper describes, in detail, a head up display (HUD) format developed at NASA Ames Research Center to provide pilots of V/STOL aircraft with complete flight guidance and control information for Category-IIIC terminal-area flight operations. These flight operations cover a large spectrum, from STOL operations on land-based runways to VTOL operations on small ships in high seas. Included in this description is a complete geometrical specification of the HUD elements and their drive laws. The principal features of this display format are the integration of the flightpath and pursuit guidance information into a narrow field of view, easily assimilated by the pilot with a single glance, and the superposition of vertical and horizontal situation information. The display is a derivative of a successful design developed for conventional transport aircraft. The design is the outcome of many piloted simulations conducted over a four-year period. Whereas the concepts on which the display format rests could not be fully exploited because of field-of-view restrictions, and some reservations remain about the acceptability of superimposing vertical and horizontal situation information, the design successfully fulfilled its intended objectives.

INTRODUCTION

It is well known that, even in an aircraft with good fixed-operating-point handling qualities, the pilot's perception of the difficulty of performing specific tasks can be sensitive to the technique used to display situation and guidance information. This sensitivity increases rapidly as the operating environment deteriorates, eventually reaching the point where not only the method of display presentation, but also the style of information representation (display format) becomes critical.

Over the past twenty years the head up display (HUD) method of display presentation has passed from being an acceptable alternative to being a preferred one. This has occurred largely because of improvements in field of view and in the sensor quality needed to maintain accurate conformability with the outside visual scene. In concert with the improved HUD technology, there has been considerable progress in understanding and developing geometrical formats for displaying the information. This effort has been accompanied by a significant conceptual change.

Early attempts at HUD display formats tended to mimic the electromechanical attitude director indicator (ADI). Flight guidance was provided by flight directors in the form of error bars that moved relative to an aircraft-body-fixed reference symbol. Surrounding this datum was an array of flight status information. The primary problem with this arrangement was that the flight guidance

---

* Simulator Applications Engineer employed by SYRE Corp., Moffett Field, California.

1

information tended to be disassociated from the status information. The danger in this was that the pilot could easily concentrate on "zeroing out" the flight-director bars to the total exclusion of any status monitoring. It follows that the potential for flying the aircraft into a hazardous situation was built into the concept. A solution to this problem, and one that is easier to implement with an electronic display than with an electromechanical one, is to integrate the guidance and flight-critical status information so that pilot awareness of aircraft status is intrinsic. This is the conceptual change referred to earlier.

The primary technique used to achieve guidance and status integration is to redirect pilot attention away from the somewhat arbitrary body-fixed datum, used in ADI-type formats, to the aircraft's velocity vector; and to adopt guidance techniques based on pursuit rather than compensatory, or flight-director, tracking. The advantage of this approach is that it duplicates well-established piloting practice. Such practice lays stress on the importance of looking where the aircraft is going rather than where it is pointing, and of being aware not only of the tracking error, but also of the motion of the tracked object and the change of aircraft state required to track it. The latter features are fundamental to pursuit tracking. One of the most successful HUD formats which follows the new philosophy was developed by Bray (ref. 1), and has been certified for commercial transport operations in Category-IIIA visibility. The pursuit display concept has also been applied to powered-lift STOL aircraft by Hynes et al. (ref. 2), and tested, both "head up" and "head down," on the Ames Research Center's Quiet Short-Haul Research Aircraft. The primary conclusion was that the concept "provided well-conditioned guidance commands for following the reference approach paths and for maintaining situation awareness under a complex instrument flight environment."

Research has been carried on for several years to devise and evaluate HUD formats designed for the VTOL approach and shipboard landing task (refs. 3-5). From this work, a format has emerged which appears to satisfy display requirements suitable for V/STOL terminal-area operations to and from small ships, operating in high seas, in Category-IIIC visibility. This format relies heavily on that of references 1 and 2 for the approach phase, and on an Army-sponsored helicopter display concept (ref. 6) that uses a horizontal velocity predictor for the hover and vertical landing phases. The major contribution of the resulting format rests in blending these concepts in a more or less consistent manner.

Simulation efforts to integrate and refine the concepts involved three piloted evaluations on the NASA Ames Research Center's Vertical Motion Simulator (VMS). Each of these simulations was preceded by extensive engineering analysis and refinement on a fixed-base simulator. This "pilot-in-the-loop" workstation was a valuable tool for generating and developing new ideas. Eleven test pilots from NASA, the Royal Aerospace Establishment, industry, and the military were involved in the evaluation process. These pilots, and numerous engineers, provided valuable suggestions.

The HUD format will be described in detail. The geometry of all the elements is defined consistent with an assumed field of view 16° wide by 16° high. All the symbol drive laws are given in general form, along with a set of drive-law constants appropriate for an AV-8A Harrier. The geometric specifications of the landing pad are similar to those of a Spruance-class destroyer.

2

The report is organized so that those who want to obtain an overview of the concepts without becoming involved in technical minutiae may skip the section entitled "Symbol Drive Laws" and the appendices.

HUD CHARACTERISTICS

All HUD formats are compromises resulting from the attempt to pack as much useful information as possible into the simplest, least-cluttered display. A pilot's reaction to a HUD format is necessarily highly subjective and depends strongly on his or her experience in performing the kind of task for which the HUD format was designed. Many design conjectures about HUD formats are based, somewhat loosely, on pilot comments. There is a need to place these conjectures on more scientific foundations. But this can only occur if measurements can be made to support these conjectures. Oculometers have not been capable of the less than 1° resolution required for such work, although promising new developments may soon change this. The best that can be done, currently, is to translate the least controversial conjectures into the following set of general requirements.

1. Primary guidance should be provided in simple, uncluttered, analog error form, centered on the flightpath symbol and capable of being assimilated with a single glance.

2. Guidance graphics and dynamics should be representative of a task familiar to the pilot.

3. Where possible within the constraints of the HUD field of view, the graphics should be conformal with the outside visual scene.

4. Flight and control system status information should fan out from the guidance information zone in order of decreasing importance to safety, with the primary status information within a 10° field of view.

5. All flight-envelope limits should be shown.

6. All control limits not clear from pilot-control positions or forces should be shown.

7. Clutter should be minimized by avoiding unvarying descriptors and, if the equipment permits it, by using intensity, color and occultation techniques.

8. Relative locations of the guidance and primary status information should match those of the associated pilot controls.

9. The display should provide the pilot with complete flight status information at all times.

NONCRITICAL AND BACKUP
STATUS INFORMATION
(DIGITAL)

SAFETY OF FLIGHT
STATUS INFORMATION
(ANALOG PREFERRED)

PRIMARY
GUIDANCE
INFORMATION
(ANALOG)

3 FOV

10 FOV
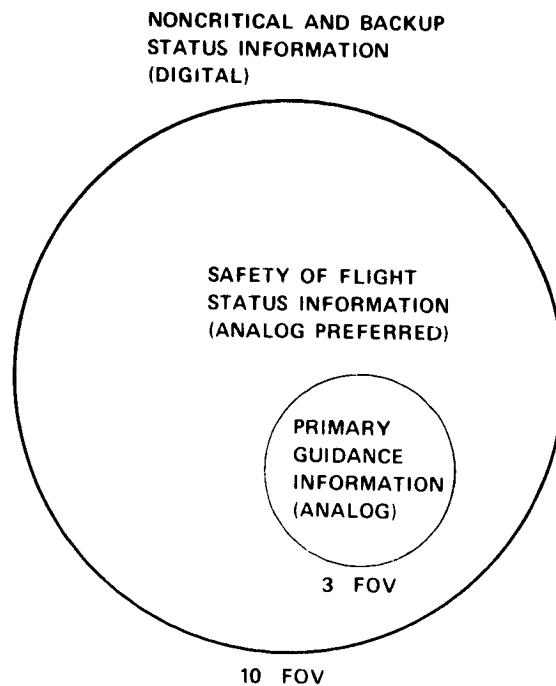
Figure 1.– HUD topology.

Requirements (1) and (4) imply a HUD topology as shown in figure 1. For the primary guidance information to be seen without eye motion, it must reside within a 3° field of view. However, this field of view may move relative to the rest of the display.

General Description

Two pilot-selectable display modes are provided, termed "approach" and "hover." Each mode has its own display format (fig. 2). Both modes are designed to be "attitude conformal," that is, elements of the display that indicate changes of attitude move in one-to-one correspondence with the outside visual references.

The approach mode can be used to make either constant-speed conventional landings, or decelerating transitions to a hover followed by a vertical landing. For either type of landing, the vertical and lateral guidance is contained in a symbol representing a "ghost" aircraft (fig. 2(a)). This symbol identifies the position of a fictitious aircraft located ahead of the real aircraft and performing the approach task perfectly. The pilot's vertical and lateral control actions are reflected in the motion of a "flightpath" symbol (fig. 2(a)). This symbol indicates the direction of the aircraft's inertial velocity vector. In operation, the pilot maneuvers the aircraft so that the flightpath and ghost aircraft symbols coincide. The aircraft is then flying along the reference flightpath.

For a conventional landing, the speed guidance symbol is in the form of a line indicating the longitudinal velocity error (fig. 2(a)). This line starts at the tip of a caret whose vertical position relative to the right wing of the flightpath symbol indicates longitudinal acceleration. To maintain

4
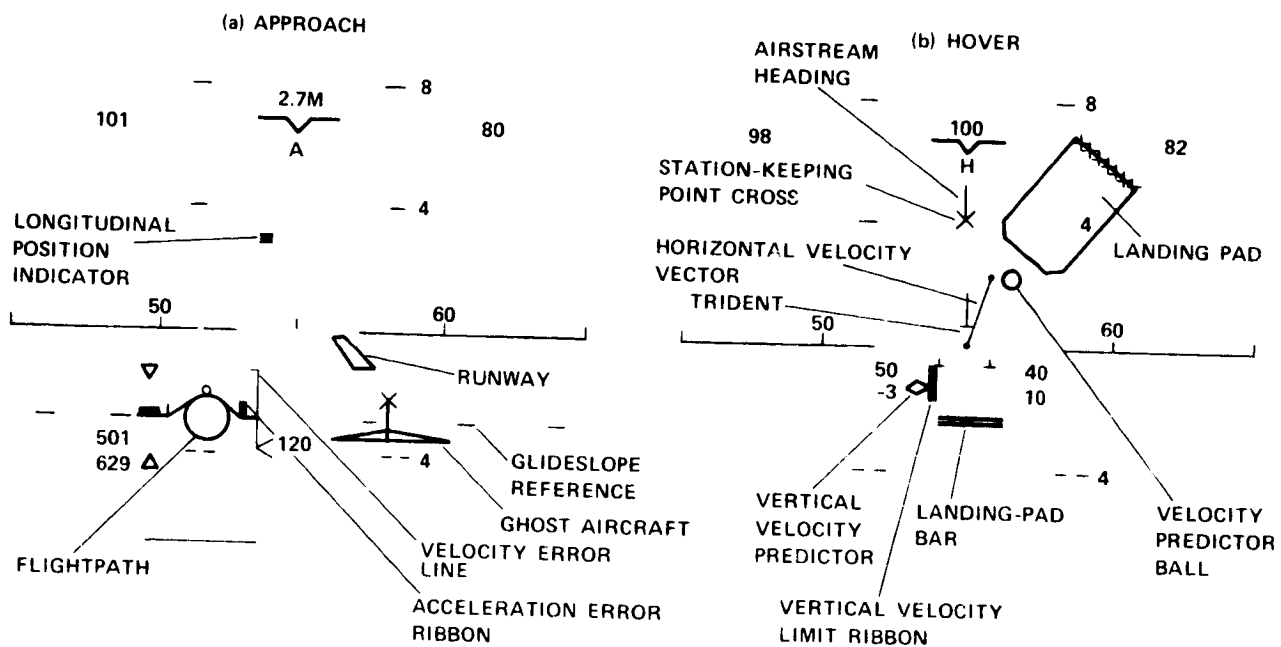
Figure 2.– Approach and hover display formats. (a) Approach; (b) hover.

constant speed, the pilot maintains the tip of the speed error line coincident with the right wing of the flightpath symbol.

For a decelerating transition to a hover, longitudinal guidance is provided in the form of a longitudinal acceleration error ribbon (fig. 2(a)). The pilot maintains a deceleration approximating that of a reference value by "nulling" this ribbon with the appropriate controls.

If the pilot has elected to make a conventional landing, a runway symbol appears on the display (fig. 2(a)), and the landing is completed using only the approach display mode.

If the pilot has elected to make a vertical landing, then, after coming to a hover at the initial station-keeping point using the approach display mode, he selects the hover display mode. This mode presents a superposition of information in both the vertical and horizontal aspects (fig. 2(b)). The central display element is a fixed "trident" symbol that is a plan-view representation of the aircraft showing the correct relative locations of the wheels and noseboom. The landing pad is presented in both the vertical and horizontal aspects. In the horizontal aspect, the pad symbol is geometrically similar to the real landing pad and is scaled in both size and relative position to match the trident. In the vertical aspect, the pad ("landing-pad bar" in fig. 2(b)) is shown edgewise at a distance below the trident proportional to the altitude above the landing pad. The primary guidance information, in hover, is contained in symbols representing the final station-keeping point, the height above the deck (landing-pad bar), and the vertical velocity allowable within a prescribed landing-gear limit. In operation, the pilot, using the appropriate controls, moves a predicted horizontal velocity symbol (fig. 2(b)) over the station-keeping point symbol and holds it there, while maintaining constant altitude. When the aircraft is at the station-keeping point, the pilot moves

5

the predicted vertical velocity symbol (fig. 2(b)) to establish a rate of descent, within the limits of the allowable vertical velocity ribbon (fig. 2(b)), until touchdown. The allowable vertical velocity ribbon is especially useful if the landing pad is moving vertically, as in the case of a ship deck.

Sensor Requirements

The display is designed for an aircraft equipped with a full inertial navigation system providing aircraft angular and translational positions, velocities, and accelerations. An air data system is required to provide true airspeed, angle of attack, sideslip, barometric altitude and altitude rate. Terminal-area navigation information requires a microwave scanning radar, distance-measuring equipment (DME) and radio altimeter. To achieve high positional accuracy in hover, additional sensors such as a laser tracker may be required. When operating onto a ship, data on the speed and direction of the ship and the wind over deck (WOD) must be uplinked to the aircraft. Depending on the severity of the ship motion, the ship may need to be equipped with an inertial navigation system providing the position, velocity, and acceleration of the desired touchdown point on the deck. This information also must be uplinked to the aircraft.

Certain pilot-selected information must be provided to the display computer, namely:

1. Runway heading

2. Runway altitude

3. Approach glideslope

4. Approach deceleration

5. Initial and final station-keeping points relative to the desired touchdown point

6. Final approach track heading

7. Ship type (landing-pad geometry)

APPROACH DISPLAY

Aircraft Fixed Symbols

The construction of the display begins with the fixed elements shown in figure 3. These elements are:

1. Aircraft reference symbol

2. Engine speed as a percentage of the nominal maximum

3. Nozzle angle in degrees

4. Range from the station-keeping point, in nautical miles for distances greater than 1 n.mi., and in feet for distances less than 1 n.mi.

5. Control mode indicator (A for approach, H for hover)
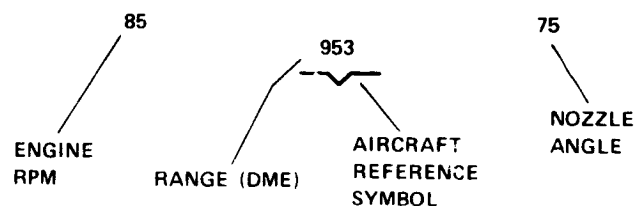
Figure 3.– Case-fixed display elements.

The gull-winged aircraft reference symbol is equivalent to the reference waterline of the aircraft. The digital readouts of engine speed and nozzle angle are removable in a HUD declutter mode selectable by the pilot.

Attitude and Flightpath References

The presentation of roll, pitch, and heading is shown in figure 4. This entire element group rolls about the aircraft reference symbol (fig. 4). The pitch scale is presented in increments of 4° relative to the horizon line. Positive pitch angles are indicated by solid bars, negative pitch angles by dashed bars. As shown in figure 5, the pitch angle is 6.5°. The heading readouts are at every 10° (fig. 4). The aircraft's heading is determined by the perpendicular from the aircraft reference symbol to the horizon. As shown in figure 6, the aircraft's heading is 55°.
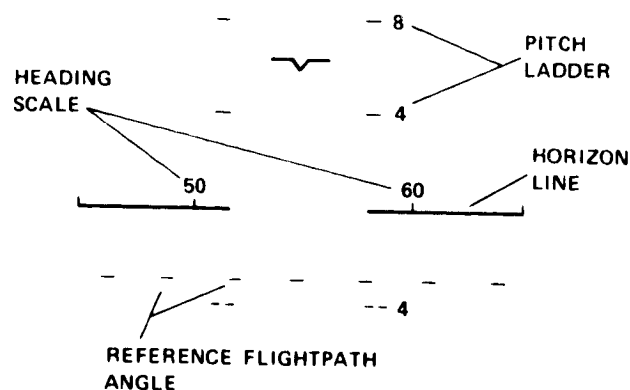
Figure 4.– Attitude cue display elements.
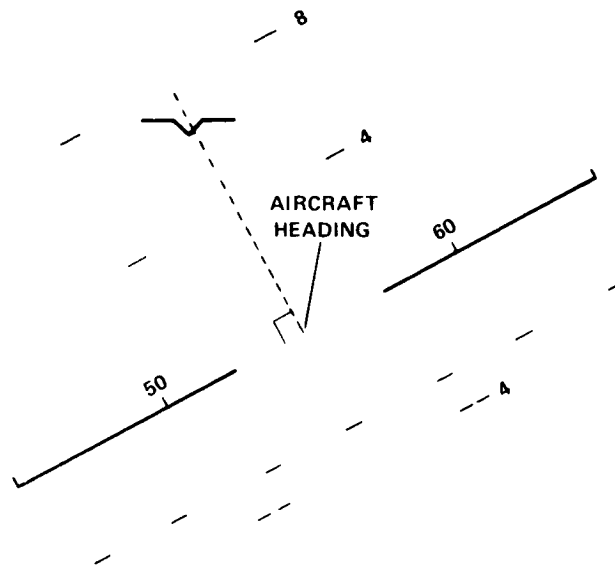
Figure 5.– Determination of aircraft heading.
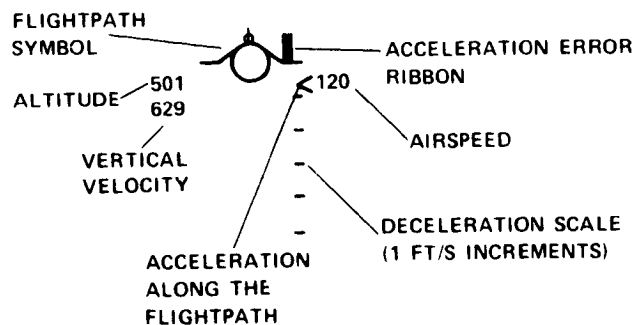
Figure 6.– Flightpath symbol and associated elements.

The flightpath reference, shown in figure 5 as a dashed line parallel to the horizon, indicates the desired approach glideslope. The position of this reference is set by the pilot. It is especially useful in visual approaches by providing a cue to start the descent. As shown in figure 4, the flightpath reference is set for a −3° glideslope.

Flightpath Symbol Group

With the exception of the flightpath reference line, which is deleted in the hover mode, the two symbol sets described above are present in all display modes. The remaining symbols to be described are present only in particular display modes. The major additional symbol set (fig. 6) used in the approach mode comprises the flightpath (velocity vector) symbol; the airspeed, altitude, and altitude rate digits; the longitudinal acceleration caret; and the longitudinal guidance error ribbon.

8

This set of symbols moves with the flightpath symbol as a group, and rolls with the aircraft. It follows that the wings of the flightpath symbol are always parallel to the aircraft reference symbol (fig. 7). This arrangement was selected to aid in indicating roll angle, and makes the digital information easier to read, especially at high roll angles.
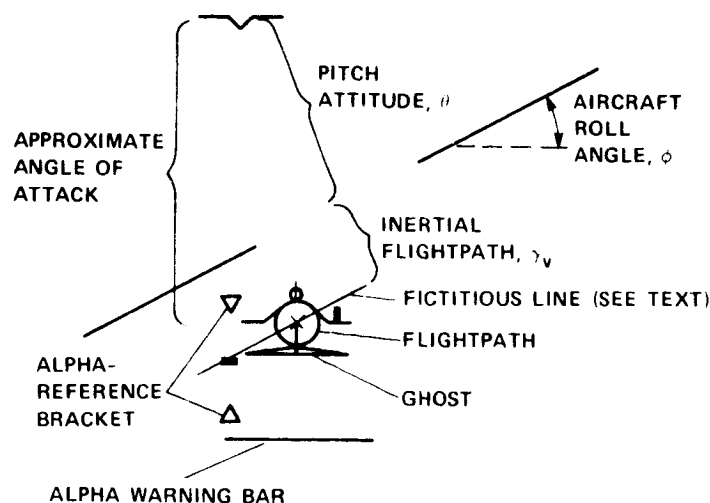
Figure 7.– Flightpath presentation in a roll.

Flightpath Symbol– The flightpath symbol is the central element of the approach and transition display and is the pilot controlled element for flight in the vertical and lateral degrees of freedom. The vertical position of the flightpath symbol relative to the horizon, read from the pitch attitude scale, is the inertial vertical flightpath angle of the aircraft. As shown in figure 2(a) the flightpath angle is $-3°$. The lateral position of the flightpath symbol shows the crosstrack angle of the aircraft, which is the difference between the aircraft's heading and its velocity vector relative to the station-keeping point. This crosstrack angle is a function of the winds and the aircraft sideslip. At low speeds the sideslip angle becomes very sensitive to changes in lateral velocity, and, in fact, flightpath angle becomes undefined at zero speed. To maintain the flightpath symbol within the HUD field of view at low airspeeds, the symbol drive laws are modified so that below a certain speed, the symbol indicates lateral and vertical velocities rather than flightpath angles. To indicate to the pilot that the change of drive law has taken place, the flightpath symbol is changed to a diamond shape (fig. 8).

Since the flightpath symbol is a primary pilot controlled element during the approach and transition, it must have response dynamics acceptable to the pilot. Unaugmented flightpath angle response to pitch, roll, or throttle changes is usually very sluggish at approach speeds, and "flying" this symbol can be difficult. This problem is overcome by adding some quickening logic to the pilot control inputs. The level of quickening employed has been found, by simulation, to significantly reduce the pilot workload, especially in the IMC (Instrument Meteorological Conditions) landing approach task.

9
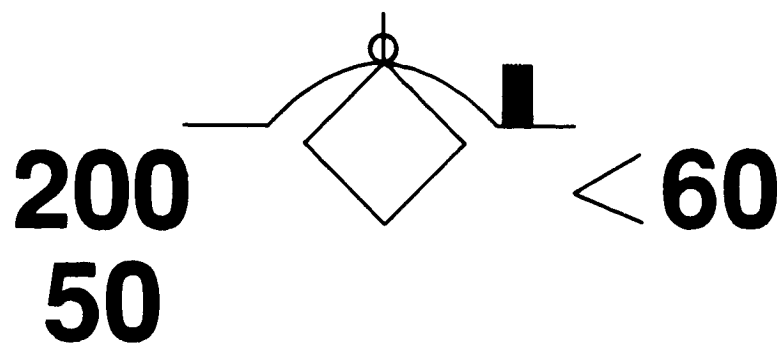
Figure 8.– Desensitized flightpath.

Digitized Flight Status– During the approach, altitude, vertical velocity, and airspeed are displayed digitally. To avoid any possibility of obscuring the flightpath symbol, these digital readouts are fixed relative to the flightpath symbol, and they therefore move with it. The readouts are close enough to the flightpath symbol so that the entire symbol group can lie within the pilot's high-definition field of view. The airspeed is in knots, updated every 1 kn; the altitude is in feet, updated every 10 ft above 200 ft and every 1 ft below 200 ft; the vertical velocity is in feet per minute, updated every 50 ft/min.

Longitudinal Acceleration– The acceleration caret (fig. 6) indicates the horizontal acceleration. This symbol is referenced to the flightpath symbol wing and, for constant speed approaches to a conventional landing, is scaled such that it can be used as a "potential flightpath angle" for energy management. For small angles, the potential flightpath is defined to be

$$\gamma_p = \frac{180}{\pi g} \dot{v}_x + \gamma \qquad (1)$$

where

γ	inertial flightpath angle
$\dot{v}_x$	longitudinal acceleration
g	acceleration due to gravity

It follows that the acceleration caret is scaled to move an angular distance on the display of 1.78° (180/πg°) for every ft/sec^2 of longitudinal acceleration. With this scaling, the position of the caret always indicates the steady-state (zero longitudinal acceleration) position of the flightpath symbol. The principal value to the potential flightpath concept is that it gives the pilot a preview of the steady-state flightpath angle and angle of attack, provided that the pitch angle and engine power setting remain constant. The concept, in essence, provides an explicit indicator of the appropriate pitch and power changes needed either to accomplish a desired maneuver or to counter an impending problem. For example, the concept provides a timely indicator of the presence of wind shear.

10

While an acceleration caret scaled to represent a potential flightpath provides useful information during conventional and STOL approaches, where longitudinal accelerations are small, its importance is diminished considerably in approaches to a vertical landing. In the latter, decelerations of 3 ft/sec^2 are nominal and may often reach 6 ft/sec^2. With decelerations of even 3 ft/sec^2, an acceleration caret with potential flightpath scaling would be 5.34° below the level of the flightpath symbol. With a nominal glideslope of −3° the acceleration caret would be 8.34° below the horizon, and therefore outside the field of view regarded as optimal for safety-of-flight monitoring. Of more practical concern is the fact that with current HUD technology the acceleration caret would be very close to the lower edge of the display, and increases of pitch angle, deceleration, or flightpath angle could easily cause the acceleration caret to move beyond the HUD field of view. These considerations have forced the abandonment of the potential flightpath concept for approaches to a vertical landing. Instead, the acceleration caret is scaled to 0.5° sec^2/ft. With this scaling the pilot can easily monitor the approach deceleration.

Longitudinal Guidance– Longitudinal, or speed, guidance is presented only if such guidance is selected by the pilot. If the pilot desires to capture and hold a given airspeed (or groundspeed), a velocity error line appears that is attached to the longitudinal acceleration caret (fig. 9(a)). This line is scaled such that if its free end always coincides with the flightpath symbol wing, a smooth convergence to the desired speed occurs. If the pilot desires to make a decelerating approach to hover, then an acceleration error ribbon is displayed (fig. 9(b)). The length of the acceleration error ribbon displays the difference between the aircraft's deceleration and the constant deceleration required to bring the aircraft to a hover at the initial station-keeping point, based on the instantaneous range and the horizontal speed.

LATERAL ACCELERATION BALL

VELOCITY
ERROR LINE

ACCELERATION
ERROR RIBBON

(a) SPEED CONTROL MODE

(b) DECELERATION
CONTROL MODE
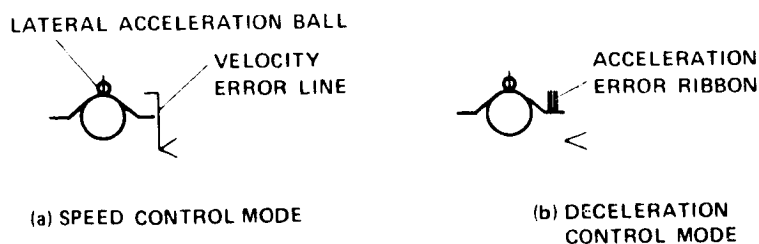
Figure 9.– Speed and acceleration control elements. (a) Speed control mode; (b) deceleration control mode.

In the final stage of transition, when the horizontal speed relative to the station-keeping point is less than 35 ft/sec, the acceleration error ribbon is automatically removed from the display and is replaced by the velocity error line (fig. 10). The length of this line is now proportional to the horizontal speed relative to the station-keeping point. An additional symbol is introduced representing the initial station-keeping point (fig. 10). The vertical distance of this symbol from the flightpath symbol represents the range from the station-keeping point. If the pilot controls the aircraft so that
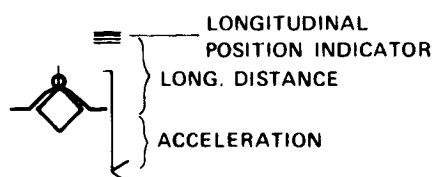
Figure 10.– Station-keeping point capture elements.

the tip of the velocity error line coincides with the station-keeping point symbol, then the aircraft will smoothly converge to the station-keeping point.

Lateral Acceleration– Lateral acceleration is indicated by a small circle that moves across the "wings" of the flightpath symbol (figs. 9, 10). This symbol is scaled such that when the circle is at the slope discontinuity of the flightpath symbol wings, the lateral acceleration is the lesser of ±0.2 g and the maximum lateral acceleration consistent with safe aircraft operation.

Angle-of-Attack References

Two angle-of-attack references are provided. One, termed the alpha warning bar, indicates excessive angle of attack. It is in the form of a horizontal bar whose vertical position relative to the aircraft reference symbol is equivalent to the maximum recommended approach angle of attack (fig. 7). This symbol translates horizontally so that its center always lies on the display fixed vertical through the flightpath symbol. The other angle-of-attack reference, termed the alpha reference bracket, is designed to provide the pilot with prominent angle-of-attack and pitch-angle references during the approach. The bracket has the orientation of the display fixed reference frame and is depressed relative to the aircraft reference symbol by a distance equivalent to the desired approach angle of attack. The nominal approach pitch angle for the AV-8A aircraft is 6.5° and the reference approach flightpath angle is −3°, resulting in a nominal approach angle of attack of 9.5°. The depression angle of the alpha reference bracket may be varied to match the characteristics of the particular aircraft. In operation, the pilot flies the aircraft so that both the flightpath symbol and ghost aircraft symbol coincide (fig. 7) and lie on a line parallel to the horizon, passing through the midpoint bar of the alpha bracket. The preferred piloting technique is to "fly" the alpha reference bracket to the ghost aircraft symbol using longitudinal stick and to fly the flightpath symbol to the ghost, using power. Essentially, this technique amounts to maintaining a constant angle of attack while controlling the flightpath with power, which is, of course, the appropriate technique for flight below the minimum-drag speed.

Consider now the situation in which the aircraft is in conventional flight, and the pilot wishes to perform a decelerating transition to a hover. In conventional flight, the pilot will most likely be controlling flightpath angle with longitudinal stick, and speed with the throttle. However, if this technique is continued in a decelerating transition to too low an airspeed, the aircraft can be flown, inadvertently, to dangerously high angles of attack. While this error is unlikely in visual conditions, in instrument conditions, when the pilot's attention is on the flightpath symbol, "alpha

12

creep" can be insidious. Simulation has shown that the presence of the angle-of-attack references is effective in providing an early warning of an inappropriate control technique during decelerating approaches.

Ghost Aircraft Symbol

The ghost aircraft symbol (fig. 2(a)) provides the vertical and lateral guidance during the approach. The symbol is in the form of a delta-wing aircraft, with a flashing beacon on the tip of the fin. The ghost aircraft can be thought of as being some distance ahead of the real aircraft and performing the approach task perfectly. By tracking the flashing beacon on the ghost with the flight-path symbol, the pilot performs a simulated pursuit task. Since it is desirable to provide constant convergence dynamics at all speeds, the ghost is maintained at a position equivalent to a constant time ahead of the real aircraft. In other words, the ghost lead distance is directly proportional to the real aircraft's inertial speed. Another important feature of the ghost is that it performs perfectly coordinated turns, thus providing the pilot with an indication of the bank angle appropriate to the reference flightpath (fig. 11).
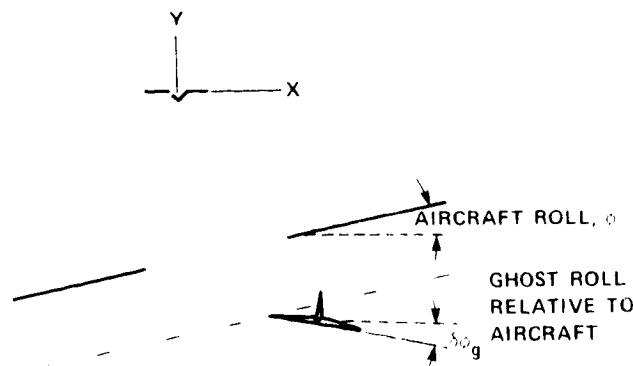
Figure 11.– Ghost aircraft rolling maneuver.

Runway Symbol

In order to provide the pilot with a greater awareness of the location of the final destination, a runway outline conformal with the real runway is provided (fig. 12). In instrument conditions, this symbol provides useful confirmation of the consistency of guidance information.

HOVER DISPLAY

Relationship to Approach Display

All the fixed elements, the horizon, and the pitch attitude ladder described for the approach display are retained for the hover display. The digital display of altitude, vertical velocity, and
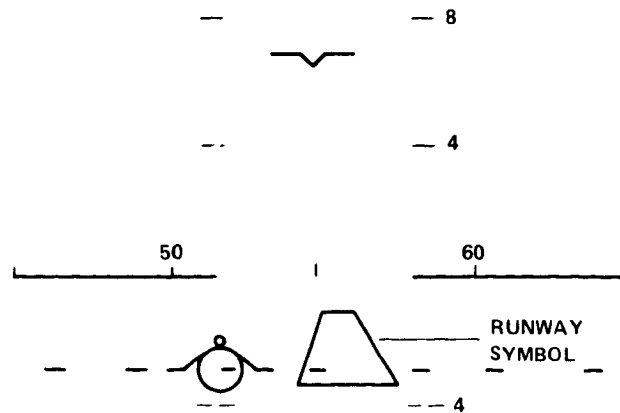
Figure 12.– Runway symbol.
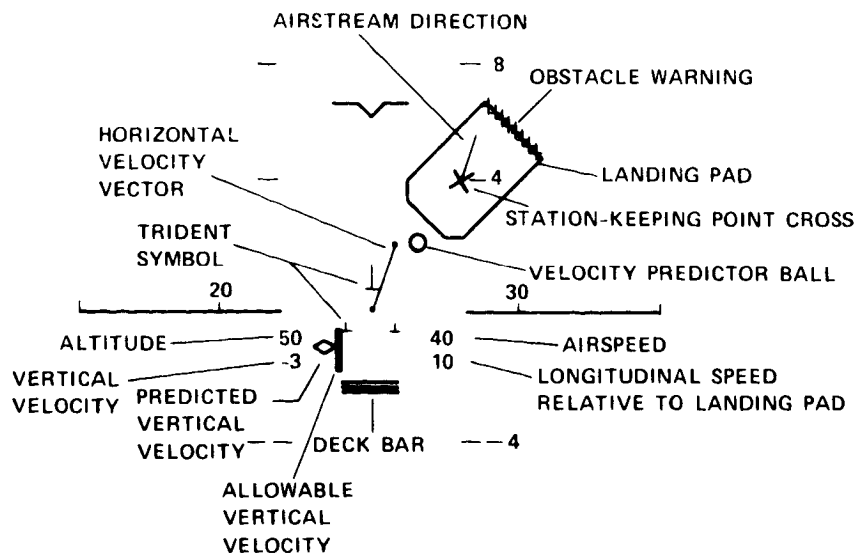
Figure 13.– Precision hover elements.

airspeed are also retained, but the vertical velocity is given in ft/sec, updated every 1 ft/sec. In addition, the longitudinal velocity relative to the station-keeping point, in kn, updated every 1 kn, is displayed below the airspeed (fig. 13). These digital readouts have a fixed location relative to the trident symbol, described below.

Additional Aircraft Fixed Elements

Whereas in the approach format the central reference symbol is the flightpath, in the hover format it is the trident symbol (fig. 13). The trident represents a plan view of the aircraft showing the relative locations of critical items such as wheels and noseboom. This symbol is depressed

14

below the aircraft reference symbol so that it lies on the horizon when the aircraft is at the landing pitch angle (6.5° for the AV-8A). All other elements specific to the hover display are referenced to the trident.

An indication of the horizontal velocity and direction relative to the landing pad is provided in the form of a vector, one end of which is fixed to the trident datum (fig. 13).

Landing Guidance Symbols

Whereas in the approach display, guidance is provided to the pilot by the ghost aircraft symbol and the longitudinal velocity and acceleration error symbols, in the hover display it is provided by the station-keeping point cross and the allowable vertical velocity ribbon (fig. 13). The station-keeping point cross indicates the position of the nominal station-keeping point (either initial or final). The initial station-keeping point is fixed relative to the mean landing-pad position, whereas the final station-keeping point is fixed relative to the landing pad itself. Attached to the station-keeping point cross is a WOD pointer (fig. 13). The length of the allowable vertical velocity ribbon is proportional to the maximum instantaneous vertical velocity consistent with a prescribed landing gear limit (fig. 13).

Pilot-Controlled Symbols

Whereas in the approach display the pilot-controlled symbols are the flightpath and longitudinal (speed or acceleration) error, in the hover display they are the predicted longitudinal velocity ball and the predicted vertical velocity diamond (fig. 13). The predicted horizontal velocity ball provides the pilot with quickened horizontal velocity with respect to the mean position of the landing pad. In fact, for many control systems, the distance between the ball and the tip of the horizontal velocity vector (fig. 13) may be interpreted as the horizontal acceleration of the aircraft. It follows that the symbol is useful for trimming the aircraft in hover. To perform an approach to the final station-keeping point, the pilot controls the position of the ball so that it leads the velocity vector in the direction of the station-keeping point cross. In the final phase of station-keeping point capture, the position of the ball is maintained coincident with the station-keeping point cross.

The predicted vertical velocity diamond provides information in the vertical degree of freedom analogous to that provided by the ball in the horizontal degrees of freedom. The piloting task for the descent to a vertical landing is to maintain the ball over the station-keeping point cross while controlling the diamond so that it always lies within the allowable vertical velocity ribbon. With this guidance and control the pilot is assured that landing-gear limits will not be exceeded at touchdown.

In the case where the aircraft control system provides translational velocity command in hover, the ball and diamond simply indicate the horizontal and vertical velocities commanded by the pilot. In other words, the positions of the ball and the diamond are in one-to-one correspondence with the positions of the appropriate pilot controls.

15

Landing-Pad Symbols

The landing pad is represented in both horizontal and vertical aspects (fig. 13). The horizontal representation is geometrically similar to the real landing pad and is scaled in both size and location to match the trident. In essence, the pilot is presented with a bird's-eye view of the landing situation. Any obstacle close to the landing pad (such as a hangar) is marked with a series of crosses (fig. 13) that flash if any part of the aircraft passes within a predetermined distance (say 10 ft) from the obstacle.

In its vertical aspect, the landing pad is represented by the landing-pad bar (fig. 13). The distance from the landing-pad bar to the base of the trident is proportional to the altitude above the deck. The landing-pad bar is useful in indicating to the pilot, during the final stage of the vertical landing, the appropriate time to increase his or her level of concentration on the task of maintaining the predicted vertical velocity diamond within the span of the allowable vertical velocity ribbon.

SYMBOL DRIVE LAWS

Preliminary Comments

The equations governing the positions of some of the display symbols are dependent on the aircraft's flying qualities and, in particular, on the type of control system augmentation. The aircraft dependent equations presented here are tailored to the AV-8A Harrier.

Some of the variables used in the equations are dependent on the reference flightpath definition. For completeness, the reference flightpath definition used in the piloted simulations leading to the HUD design described here is given in appendix B. Values of all the constants used in the symbol drive equations are given in table 1.

The headings of the following sections, which deal with the drive equations for the various symbols, are accompanied by letters A or H, or both, to indicate the display mode(s) in which the particular symbol is used.

Display Coordinate System

The origin of the display coordinate system is located at the aircraft reference symbol. A general coordinate pair is designated (X, Y), in degrees, with appropriate subscripts to identify particular symbols. To distinguish the display coordinate system from all others, the display horizontal coordinate will always be referred to as the "abscissa" and the vertical coordinate as the "ordinate."

Horizon Line and Pitch Ladder (A,H)

Since the horizon line and the pitch ladder are fixed relative to each other, they can be treated as a single symbol. The angle, ϕ, of the horizon to the display abscissa is the aircraft's roll angle (fig. 14). The coordinates of the center of the horizon (X_h, Y_h) are given by

16

TABLE 1.– DRIVE LAW CONSTANTS USED IN AV-8A HARRIER SIMULATIONS

Parameter	Value	Units	Parameter	Value	Units
A	14.0	deg	T_u	5.0	sec
A_{δ_t}	0.3	ft/deg sec^2	$T_{\dot{v}}$ ($I_{at} = 1$)	1.11	sec
D_c	1000.0	ft	$T_{\dot{v}}$ ($I_{at} = 0$)	2.0	sec
H	82.0	ft	T_{ϕ_g}	15.0	sec
$\dot{H}$	−9.0	ft/sec	V_a	100.0	ft/sec
K_{ax}	0.5	deg sec^2/ft	$\dot{V}_f$	−1.5	ft/sec
K_{ay}	5.0	deg/g	$\dot{V}_i$	−3.0	ft/sec
K_l	0.05882	deg/ft	V_{vl}	35.0	ft/sec
K_{la}	0.03	deg/ft	$V_{f_{min}}$	90.0	ft/sec
K_h	0.05882	deg/ft	$V_{f_{max}}$	100.0	ft/sec
K_u	0.2	deg sec/ft	$V_{t_{min}}$	100.0	ft/sec
K_{ua}	0.2	deg sec/ft	X_{max}	7.0	deg
K_w	0.2	deg sec/ft	Y_{min}	−13.0	deg
K_{δ_x}	3.45	ft/in. sec	Y_{max}	1.0	deg
K_{δ_y}	3.45	ft/in. sec	Γ	−3.0	deg
K_{δ_t}	0.4	ft/deg sec	ΔT_f	35.0	sec
K_c	0.3		ΔT_{gh}	10.0	sec
K_{θ_c}	3.45	ft/deg sec	ΔT_{gy}	10.0	sec
K_{ϕ_c}	3.45	ft/deg sec	ΔD_b	500.0	ft
K_{ϕ_g}	0.1		ΔD_c	500.0	ft
$K_{\dot{\theta}}$	0.25	ft/deg sec	Θ	6.5	deg
$K_{\dot{\phi}}$	1.75	ft/deg sec	Σ_u	0.05	1/sec
L_g	5.0	ft	Σ_v	0.05	1/sec
R	8000.0	ft	Σ_w	0.02	1/sec
S_x	−100.0	ft	Σ_u'	0	1/ft
S_y	−100.0	ft	Σ_v'	0	1/ft
T_1	2.5	sec	Σ_w'	0.00164	1/ft
T_2	10.0	sec	Σ_{wc}	0.88	1/sec
T_4	5.0	sec	Σ_{wd}	0.77	1/sec
T_5	0.5	sec	Ψ	0	deg
T_6	10.0	sec	Ψ_f	0	deg
T_h	1.11	sec	Ψ_i	60.0	deg

$$\dot{X}_h = \theta \sin \phi \tag{2}$$

$$Y_h = -\theta \cos \phi \tag{3}$$

where θ is the pitch angle (fig. 14).
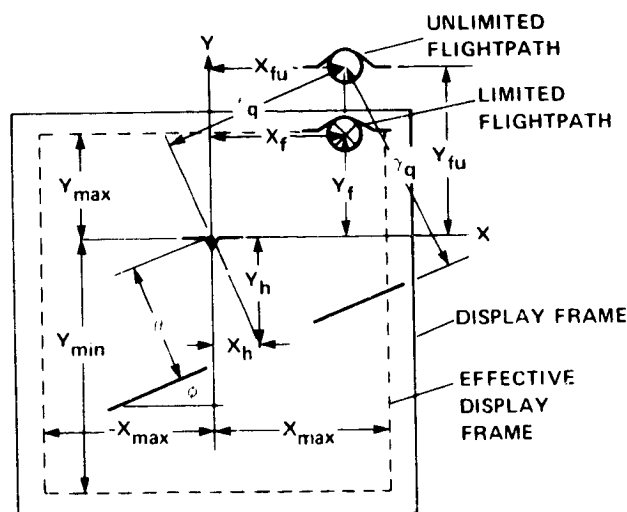
Figure 14.– Flightpath and horizon coordinates.

Reference Glideslope (A)

The glideslope reference consists of a dashed line (fig. 2(a)) parallel to the horizon and displaced from the horizon by the reference glideslope, Γ. Although all the simulations were performed using a constant reference glideslope, this is not a fundamental restriction of the concept.

Flightpath (A)

The wings of the flightpath symbol are always parallel to the display abscissa. The vertical flightpath angle, γ, relative to a coordinate frame of reference that is parallel to the earth fixed axis system, but moving at the constant horizontal velocity of the station-keeping point (fig. 15), is given by

$$\gamma = \frac{180}{\pi} \arctan \left(\frac{\dot{h}}{v_t} \right) \tag{4}$$

where

18

$\dot{h}$ inertial vertical velocity of the aircraft

v_t inertial horizontal velocity measured with respect to the station-keeping point (fig. 15)

The inertial horizontal velocity, v_t, is given by the equation

$$v_t = \sqrt{v_n{}^2 + v_e{}^2} \tag{5}$$

where v_n and v_e are the north and east velocities measured in the inertial reference frame moving with the station-keeping point.
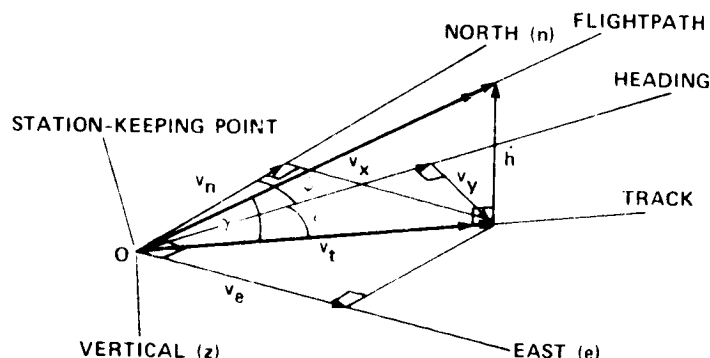
Figure 15.– Flightpath angle definition.

During an approach to a vertical landing, as the airspeed decreases, the effectiveness of pitch and power changes on flightpath angle and airspeed vary considerably. At the higher speeds (greater than 120 kn) the pilot prefers to use pitch rather than power to change the flightpath (front side technique), because of the smaller response time. However, even using pitch the response time can be exessive, and significant pilot compensation is required to achieve a desired flightpath angle. The pilot compensation can be reduced by quickening the flightpath symbol's response to pitch changes so that the symbol gives the pilot a preview of the steady-state flightpath angle corresponding to a pitch change. One way to achieve this effect is to add to equation (4) a term proportional to washed-out pitch rate. At low airspeeds (less than 120 kn), pitch gradually becomes a poor controller of flightpath, because large pitch changes produce only small steady-state changes of flightpath and, at high angles of attack, these changes can be in the reverse direction to those that occur at high airspeed. In fact, at airspeeds below about 60 kn, it is appropriate to remove the pitch quickening term. At speeds below about 100 kn, the pilot prefers to change his control technique to one of using power rather than pitch to change the flightpath angle (back side technique). Again, because of the slow response of the flightpath to power changes, pilot compensation can be reduced by replacing the rate of climb in equation (5), by a variable that gives the pilot a preview of the commanded

19

steady-state rate of climb. This can be done either by using commanded rate of climb, if the control system permits, or by adding to the measured rate of climb a term proportional to the estimated vertical acceleration resulting from throttle input. The resulting quickened flightpath angle, γ_q, is given by

$$\gamma_q = \frac{K_{\dot\theta} k_{\dot\theta} \dot\theta}{s + \sigma_w} + \frac{180}{\pi} \arctan\left(\frac{\widehat{\dot{h}_c}}{v_{tl}}\right) \tag{6}$$

where

$K_{\dot\theta}$	pitch rate gain
$k_{\dot\theta}$	pitch rate blending gain
$\dot\theta$	pitch rate
s	Laplace transform variable
σ_w	heave damping constant
$\widehat{\dot{h}_c}$	estimated commanded vertical velocity
v_{tl}	limited longitudinal velocity

The pitch rate blending gain, $k_{\dot\theta}$, is varied linearly from unity above an airspeed of $V_{f_{max}}$ to zero below an airspeed of $V_{f_{min}}$ as follows:

$$k_{\dot\theta} = \begin{cases} 1 & \text{if } v_{af} > V_{f_{max}} \\ (v_{af} - V_{f_{min}})/(V_{f_{max}} - V_{f_{min}}) & \text{if } V_{f_{max}} \geq v_{af} \geq V_{f_{min}} \\ 0 & \text{if } v_{af} < V_{f_{min}} \end{cases} \tag{7}$$

where

v_{af}	filtered airspeed
$V_{f_{min}}$	preset minimum value of v_{af}
$V_{f_{max}}$	preset maximum value of v_{af}

A first-order filter is used to smooth the measured airspeed, v_a, thus:

$$v_{af} = \frac{v_a}{T_1 s + 1} \tag{8}$$

where T_1 is the filter time constant.

The pitch rate gain, $k_{\dot\theta}$, is varied with filtered airspeed (eq. (7)), to approximately match the sensitivity of the flightpath angle to pitch-angle changes.

The heave damping parameter, σ_w, is given by the equation

$$\sigma_w = \Sigma_w + v_{af} \Sigma_w' + \Sigma_{wd} I_d \tag{9}$$

where

Σ_w	estimate of the aircraft's heave damping parameter in hover ($v_{af} = 0$)
Σ_w'	estimate of the average rate of change of the heave damping parameter with airspeed over the approach airspeed range
Σ_{wd}	heave damper constant
I_d	heave damper engage indicator

Equation (9) accounts for the effect of a heave damper mode operating through the engine. If a damper is available and is engaged, then $I_d = 1$; otherwise $I_d = 0$.

The quickened vertical velocity, $\widehat{h}_c$, used in equation (5) is obtained by adding to the measured vertical velocity a term proportional to washed-out pilot control input. If the control system is operating in either a flightpath or a vertical velocity command mode ($I_w = 1$), then

$$\widehat{h}_c = \dot{h} + \frac{s\dot{h}_c}{s + \Sigma_{wc}} \qquad \text{if } I_w = 1 \tag{10}$$

where

$\dot{h}_c$	commanded vertical velocity
Σ_{wc}	damping constant of the vertical velocity command mode

If altitude is controlled directly through the throttle ($I_w = 0$), as with the basic AV-8A, then

$$\widehat{h}_c = \dot{h} + \frac{k_{\delta_t} s \delta_t}{s + \sigma_w} \qquad \text{if } I_w = 0 \tag{11}$$

where

δ_t	throttle position
k_{δ_t}	throttle washout gain

The throttle washout gain, k_{δ_t}, is determined by the requirement that the change of steady-state vertical velocity be approximately equal to the change of throttle position multiplied by k_{δ_t}. An acceptable value for k_{δ_t} is given by

$$k_{\delta_t} \approx \frac{A_{\delta_t}}{\sigma_w} \sin \theta_j \tag{12}$$

where

A_{δ_t} change of gross thrust per unit mass of the
           aircraft per unit change of throttle position

θ_j engine nozzle angle; defined as $0°$
           when the nozzles point aft

For the AV-8A, it has been found adequate to make A_{δ_t} a constant (0.3 ft/deg sec^2) over the normal approach speed range (0-120 kn). However, at low speeds it has been found necessary to limit the value of k_{δ_t} to avoid oversensitivity of the flightpath symbol to throttle inputs, thus

$$\text{if} \quad k_{\delta_t} \geq K_{\delta_t}, \quad \text{then} \quad k_{\delta_t} = K_{\delta_t} \tag{13}$$

Furthermore, to avoid excessive sensitivity of the flightpath symbol at low speeds, a limited horizontal speed, v_{tl}, is used in equation (6). This limited speed is given by

$$v_{tl} = \begin{cases} v_t & \text{if } v_t \geq V_{t_{min}} \\ V_{t_{min}} & \text{if } v_t < V_{t_{min}} \end{cases} \tag{14}$$

It follows that when $v_t < V_{t_{min}}$, the flightpath symbol responds to changes of vertical velocity rather than flightpath angle. The pilot is alerted to the switch to a desensitized flightpath symbol by a change of symbol shape from a circle to a diamond (figs. 7, 8). The limit speed, $V_{t_{min}}$, is inversely proportional to the desired sensitivity of the symbol at low speed. Experience has shown a sensitivity of about $0.6°$ of movement on the display per foot per second of aircraft vertical velocity to be satisfactory.

The lateral inertial flightpath angle, ϵ, (fig. 15) is given by the equation

$$\epsilon = \frac{180}{\pi} \arcsin\left(\frac{v_y}{v_t}\right)$$

where v_y is the lateral inertial velocity of the aircraft relative to the station-keeping point, given by

$$v_y = v_e \cos \psi - v_n \sin \psi$$

and where ψ is the heading (fig. 15).

The lateral response of the flightpath symbol to pilot commands is quickened by adding to the lateral velocity a term proportional to roll rate, as follows:

22

$$\epsilon_q = K_\epsilon \frac{180}{\pi} \arcsin \left(\frac{v_y + K_\phi \dot{\phi}/(s + \sigma_v)}{v_{tl}} \right) \qquad (15)$$

where

$\dot{\phi}$	roll rate
K_ϕ	lateral response quickening gain
K_ϵ	lateral scaling gain
σ_v	lateral velocity damping parameter

It should be noted that the limited horizontal speed (eq. (14)) is used in equation (15) to desensitize the lateral motion of the flightpath symbol, at low speed, in the same way that vertical motions are desensitized.

The lateral velocity damping parameter, σ_v, like σ_w, is made a linear function of the filtered airspeed, thus

$$\sigma_v = \Sigma_v + v_{af} \Sigma_v' \qquad (16)$$

where

Σ_v	estimate of the aircraft's lateral damping parameter in hover ($v_{af} = 0$)
Σ_v'	estimate of the average rate of change of the lateral velocity damping parameter with airspeed, over the approach airspeed range

To calculate the display drive signals, it is necessary to transform the quantities γ_q and ϵ_q into the display frame of reference, scale the resultant quantities appropriately, and limit the final values so that the flightpath symbol is always on the display. The equations for the unlimited flightpath drive signals are

$$X_{fu} = \epsilon_q \cos \phi - (\gamma_q - \theta) \sin \phi$$
$$Y_{fu} = \epsilon_q \sin \phi + (\gamma_q - \theta) \cos \phi \qquad (17)$$

The values of X_{fu} and Y_{fu} are limited so that the flightpath symbol never moves closer than 1° from the edge of the display. The following equations provide this limiting function and complete the specification of the flightpath symbol display coordinates.

23

$$X_f = \begin{cases} X_{fu} & \text{if } |X_{fu}| < X_{max} \\ X_{max} \text{ sign}(X_{fu}) & \text{if } |X_{fu}| \geq X_{max} \end{cases}$$

$$Y_f = \begin{cases} Y_{fu} & \text{if } Y_{min} < Y_{fu} < Y_{max} \\ Y_{min} & \text{if } Y_{fu} \leq Y_{min} \\ Y_{max} & \text{if } Y_{fu} \geq Y_{max} \end{cases} \quad (18)$$

The flightpath symbol coordinates are shown in figure 14, which also shows that when the flightpath symbol is limited, the pilot is alerted by the addition of a cross to the flightpath symbol circle.

Ghost Aircraft (A)

The elevation angle of the ghost aircraft relative to the real aircraft, η_g, is given by the equation

$$\eta_g = \frac{180}{\pi} \text{ arctan} \left(\frac{h_g - h}{\delta x_{gh}} \right) \quad (19)$$

where

h_g	height of the ghost aircraft
h	height of aircraft
δx_{gh}	lead distance of the ghost aircraft for the vertical tracking task

To keep the closure dynamics roughly constant, the ghost lead distance, δx_{gh}, is made proportional to the horizontal speed. To avoid the singularity that would occur in equation (19) if δx_{gh} were to become zero in hover, δx_{gh} is made proportional to the limited horizontal speed, v_{tl} (eq. (14)):

$$\delta x_{gh} = v_{tl} \, \Delta T_{gh} \quad (20)$$

where ΔT_{gh} is the ghost lead time for the vertical tracking task.

Since the ghost aircraft is assumed to be on the constant reference glideslope, Γ, its altitude, h_g, may be expressed as follows:

$$h_g = \begin{cases} H - (d - \delta x_{gh} \, k_{wg}) \tan \Gamma & \text{if } d \geq \delta x_{gh} \, k_{wg} \\ H & \text{if } d < \delta x_{gh} \, k_{wg} \end{cases} \quad (21)$$

where

H	reference hover altitude
Γ	reference flightpath angle

24

d	distance of the aircraft from the station-keeping point, measured along the reference flightpath ground track
k_{wg}	ghost lead blending gain

The purpose of the ghost lead blending gain, k_{wg}, is to ensure that when the velocity v_t becomes zero (hover), the ghost aircraft is at the hover altitude. The equation for k_{wg} is

$$k_{wg} = \begin{cases} 1 & \text{if } v_t > v_{tl} \\ v_t/v_{tl} & \text{if } v_{tl} \geq v_t \geq 0 \\ 0 & \text{if } v_t < 0 \end{cases} \tag{22}$$

To provide horizontal guidance to the predetermined curved flightpath, the ghost aircraft must appear to be located on the tangent to the flightpath at the aircraft's location (fig. 16). It follows from the geometry of figure 16 that the azimuth angle of the ghost aircraft relative to the longitudinal axis of the aircraft, μ_g, is given by the equation

$$\mu_g = K_\epsilon \left[(\psi_t - \psi) k_{wg} + \delta_{\mu_s} \right] - \frac{180}{\pi} \arctan \left(\frac{\delta y}{\delta x_{gy}} \right) \tag{23}$$

where

ψ	aircraft heading
ψ_t	heading of the tangent to the reference flightpath track (fig. 16)
δy	lateral distance of the aircraft from the reference flightpath track (fig. 16)
δx_{gy}	distance of the ghost aircraft ahead of the real aircraft for the lateral tracking task (fig. 16)
δ_{μ_s}	correction to provide turn coordination at turn entry and exit

The lead distance, δx_{gy}, is calculated similarly to δx_{gh}, thus

$$\delta x_{gy} = v_{tl} \, \Delta T_{gy} \tag{24}$$

where ΔT_{gy} is the ghost lead time for the lateral tracking task.

It should be noted here that the ghost lead distances δx_{gh} and δx_{gh} are not necessarily equal, their values being set by the aircraft's vertical and lateral control dynamics and the required closure dynamics.

With crosswinds and a control technique aimed at maintaining low values of lateral acceleration, the crosstrack angle, $(\psi_t - \psi)$, can become as high as 45°. To avoid lateral limiting of the ghost aircraft on the display, it is necessary to multiply the crosstrack angle by the lead blending gain, k_{wg}, (eq. (22)).

25
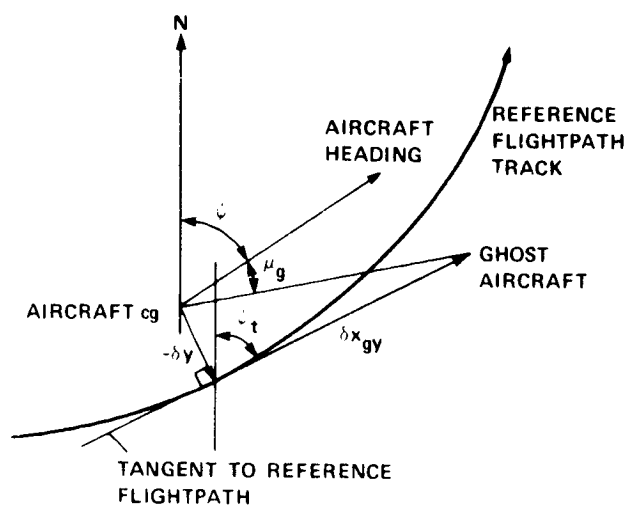
Figure 16.– Lateral ghost position.

The display coordinates of the ghost aircraft symbol are calculated in the same manner as for the flightpath symbol. The resulting equations for the unlimited ghost symbol coordinates are

$$X_{gu} = \mu_g \cos \phi - (\eta_g - \theta) \sin \phi$$
$$Y_{gu} = \mu_g \sin \phi + (\eta_g - \theta) \cos \phi$$

(25)

The ghost aircraft symbol is subject to the same display size limits as the flightpath angle. The following equations complete the ghost symbol position specification.

$$X_g = \begin{cases} X_{gu} & \text{if } |X_{gu}| < X_{max} \\ X_{max} \, \text{sign}(X_{gu}) & \text{if } |X_{gu}| \geq X_{max} \end{cases}$$
$$Y_g = \begin{cases} Y_{gu} & \text{if } Y_{min} < Y_{gu} < Y_{max} \\ Y_{min} & \text{if } Y_{gu} \leq Y_{min} \\ Y_{max} & \text{if } Y_{gu} \geq Y_{max} \end{cases}$$

(26)

As stated earlier, the ghost aircraft symbol indicates to the pilot the angle of bank required to follow the flight path laterally. This feature is particularly useful when entering or leaving a curved segment of the flightpath, since the ghost can be programmed to give some lead information and thereby minimize any tendency to overshoot or undershoot at the turn entry and exit. The equation used for the ghost aircraft angle of bank, ϕ_g, is

$$\phi_g = \frac{180}{\pi} i k_\phi \, \arctan \left(\frac{v_t^2}{Rg} \right)$$

(27)

where

26

	indicates whether the local reference flightpath is

i — indicates whether the local reference flightpath is straight ($i = 0$) or curved, and if curved, whether to the right ($i = +1$) or to the left ($i = -1$)

k_ϕ — turn entry or exit blending function

R — radius of curvature of the reference flightpath track

and the ghost aircraft angle of bank relative to the real aircraft (fig. 11), $\delta\phi_g$, is

$$\delta\phi_g = \phi_g - \phi \tag{28}$$

The blending function, k_ϕ, ramps the ghost aircraft bank angle in or out over preset distances, to provide a smooth turn entry and exit (fig. 17), and is defined by the equations

$$k_\phi = \begin{cases} 0 & \text{if } d \geq D_b + \Delta D_b \\ \frac{D_b + \Delta D_b - d}{\Delta D_b} & \text{if } D_b + \Delta D_b > d \geq D_b \\ 1 & \text{if } D_b > d \geq D_c + \Delta D_c \\ \frac{d - D_c}{\Delta D_c} & \text{if } D_c + \Delta D_c > d \geq D_c \\ 0 & \text{if } d < D_c \end{cases} \tag{29}$$

where

D_b, D_c — ranges at curved flightpath entry and exit

$\Delta D_b, \Delta D_c$ — lead blend distances at curved flightpath entry and exit

In addition, to make the ghost aircraft's position and bank angle consistent with a coordinated turn at the turn entry and exit, it is nessesary to include the correction term δ_{μ_g} in equation (23). It has been found to be adequate to represent δ_{μ_g} by a suitably scaled, washed-out ghost aircraft bank angle, thus

$$\delta_{\mu_g} = \frac{K_{\phi_g} s\phi_g}{T_{\phi_g} s + 1} \tag{30}$$

where

K_{ϕ_g} — washout gain

T_{ϕ_g} — washout time constant

27
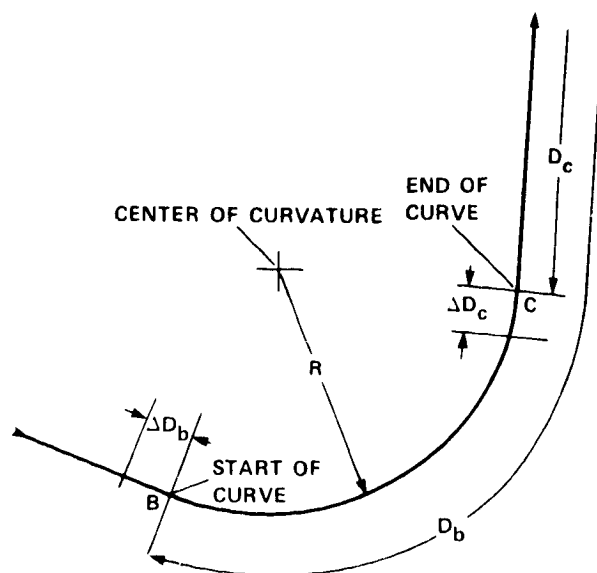
Figure 17.– Ghost bank angle blend geometry.

Values for K_{ϕ_g} and T_{ϕ_g} have been found (table 1) which keep the lateral tracking error to less than 8 ft during turn entry and exit, provided the pilot keeps the ghost aircraft symbol beacon close to the center of the flightpath symbol. Furthermore, the motion of the ghost aircraft symbol itself appears to the pilot to be well coordinated.

Angle-of-Attack Warning Bar (A)

The angle-of-attack warning bar is positioned on the display (fig. 18) such that if the flightpath symbol passes below this bar, then the operational maximum angle of attack has been exceeded. The problem here is that the angular distance between the aircraft reference and flightpath symbols is equal to the true angle of attack only if the air mass is moving at the same constant horizontal speed as the station-keeping point, and then only if the roll angle is small. Therefore, if the angle-of-attack warning bar were to be located at a fixed distance (in degrees) relative to the aircraft reference symbol and equal to the maximum operational angle of attack, the effects of wind shear and updrafts would not be apparent on the display. To overcome this problem, the angle-of-attack warning bar is located at a variable position, Y_{am}, relative to the aircraft reference symbol, obtained by the equation

$$Y_{am} = Y_f + (\widehat{\alpha} - A)\,k_{wg} \tag{31}$$

where

A approach maximum angle of attack

28
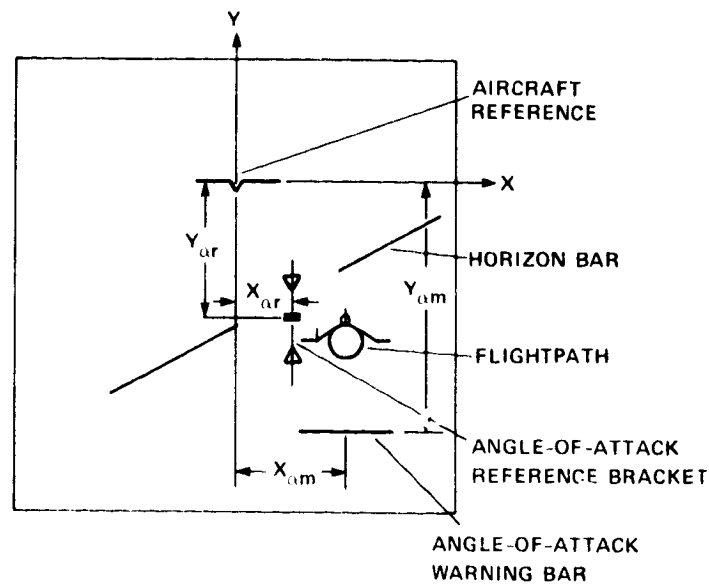
Figure 18.– Angle-of-attack warning bar and reference bracket positions.

$\widehat{\alpha}$ filtered measured angle of attack

If $\widehat{\alpha} > A$, then it follows from equation (31) that $Y_{\alpha m} > Y_f$, and the flightpath symbol is below the angle-of-attack warning bar, as required. Furthermore, equation (31) provides the correct angle-of-attack interpretation of the relative positions of the flightpath and angle-of-attack warning symbols independently of roll angle.

The filtered angle of attack, $\widehat{\alpha}$, is calculated from the equation

$$\widehat{\alpha} = \frac{\alpha}{T_1 s + 1} \tag{32}$$

where α is the measured angle of attack.

The parameter k_{wg} in equation (31) is used to desensitize the term $(\widehat{\alpha} - A)$ at low speeds, in the same way that the flightpath symbol is desensitized. At airspeeds below 30 kn the angle-of-attack warning bar ceases to be of significance and is removed from the display.

The warning bar is always parallel to both the aircraft reference and the flightpath symbols and has a lateral position, $X_{\alpha m}$, that is always the same as that of the flightpath symbol ($X_{\alpha m} = X_f$). If $Y_f < Y_{\alpha m}$, the warning bar flashes with a frequency of 3 Hz.

29

Angle-of-Attack Reference Bracket (A)

The angle-of-attack reference bracket provides a set of depressed pitch references to aid the pilot in maintaining an approximately constant angle of attack and pitch attitude during the approach. In the display coordinate system, the bracket is always parallel to the ordinate, and has a fixed horizontal position relative to the flightpath symbol (fig. 18). The equations defining the position of the center element are

$$X_{\alpha r} = X_f - 1.875$$
$$Y_{\alpha r} = -\Theta + k_{wg}\,\Gamma \tag{33}$$

Acceleration Caret (A)

The vertical displacement of the acceleration caret relative to the right wing of the flightpath symbol is proportional to some suitable measure of longitudinal acceleration. If the landing is to be conventional ($I_l = 0$), then it is presumed that the maximum thrust/weight ratio may be less than unity. In this event it is important that wing lift be maintained to touchdown. This, in turn, dictates that airspeed rather than inertial speed be maintained constant, and that acceleration relative to the air mass, $\widehat{v}_a$, be indicated on the display for use with the potential-flightpath concept. A smoothed estimate of $\dot{v}_a$, namely $\widehat{v}_a$, is calculated by complementary filtering of the inertial longitudinal acceleration, $\dot{v}_x$, and the airspeed, v_a, as follows:

$$\widehat{v}_a = \frac{T_4\,s}{T_4\,s + 1}\left(\dot{v}_x + \frac{v_a}{T_4}\right) \qquad \text{if } I_l = 0 \tag{34}$$

where T_4 is the filter time constant.

The inertial acceleration along the track, $\dot{v}_x$, is given by the equation

$$\dot{v}_x = \dot{v}_n \cos\psi + \dot{v}_e \sin\psi + (v_e \cos\psi - v_n \sin\psi)\frac{\dot{\psi}\pi}{180} \tag{35}$$

where $\dot{v}_n$ and $\dot{v}_e$ are the inertial accelerations of the aircraft in the north and east directions, respectively.

If the landing is to be vertical ($I_l = 1$), then the maximum thrust-to-weight ratio must be greater then unity, and it is assumed that any loss of wingborne lift can be compensated for by an increase of thrust. In addition, the task of decelerating to a hover at a precise point in space requires knowledge of accelerations relative to inertial space, rather than relative to the air mass. These considerations lead to the selection of $\dot{v}_x$, suitably smoothed, to be represented by the acceleration caret.

30

The position of the acceleration caret on the display, f_a (fig. 19), is

$$f_a = \begin{cases} 180\widehat{\dot{v}}_a/\pi g & \text{if } I_l = 0 \\ \\ K_{ax}\dot{v}_x/(T_5 s + 1) & \text{if } I_l = 1 \end{cases} \tag{36}$$

where

T_5 filter time constant
K_{ax} scale factor converting longitudinal accelerations to display angles

The position of the acceleration caret in display coordinates (X_a, Y_a) is

$$\begin{aligned} X_a &= X_f + 1.5 \\ Y_a &= Y_f + f_a \end{aligned} \tag{37}$$

Velocity Error Line (A)

The symbol drive law for the velocity error line (fig. 19) depends on the type of landing. For a conventional landing ($I_l = 0$), the length of the line is proportional to the difference between the airspeed, v_a, and a preset reference approach airspeed, V_a. For this type of approach, the velocity error line is displayed throughout. The pilot's task is to maintain the tip of the line coincident with the right wing of the flightpath symbol. For a vertical landing ($I_l = 1$), the velocity error line is active only when the longitudinal inertial speed, v_x, is less than some preset value V_{vl} (35 ft/sec has been shown to be satisfactory), and its length is proportional to v_x. The pilot's task is to maintain the tip of the line on the initial-station-keeping-point indicator when this symbol appears on the display. The equations defining the length, f_u, of the velocity error line (fig. 19) are

for $I_l = 0$

$$f_u = \frac{180}{\pi T_u g}(v_a - V_a) \tag{38}$$

for $I_l = 1$

$$f_u = \begin{cases} K_{ua}v_x & \text{if } v_x \leq V_{vl} \\ 0 & \text{if } v_x > V_{vl} \end{cases} \tag{39}$$

where

T_u time constant selected for the airspeed response
K_{ua} scale factor converting velocities to display angles

31

and the longitudinal inertial velocity, v_x, is determined from the equation

$$v_x = v_n \cos \psi + v_e \sin \psi$$
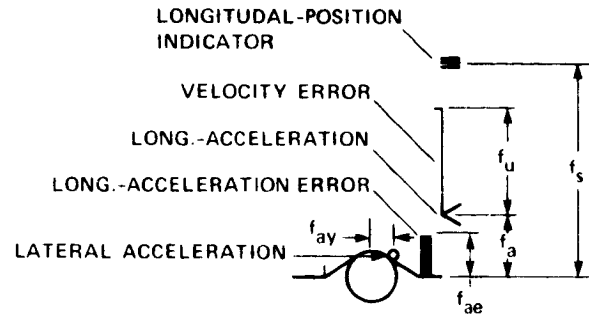
Figure 19.– Flightpath symbol referenced information.

The display coordinates of the end of the velocity error line (X_{ux}, Y_{ux}) are given by the equations

$$
\begin{aligned}
X_{ux} &= X_f + 1.25 \\
Y_{ux} &= Y_f + f_a + f_u
\end{aligned}
\tag{40}
$$

Longitudinal Position Indicator (A)

The longitudinal position indicator identifies the position of the initial station-keeping point. This symbol (fig. 19) appears on the display at the end of the approach transition, when the aircraft is within 280 ft of the initial station-keeping point. When the indicator is coincident with the right wingtip of the flightpath symbol, the aircraft's c.g. is at the station-keeping point. Since the aircraft's longitudinal control changes the velocity along the aircraft's longitudinal axis, the distance f_s (fig. 19) is made proportional to the projection of the distance from the station-keeping point onto this axis, thus

$$f_s = K_{la}[d \cos(\psi - \psi_t) - \delta y \sin(\psi - \psi_t)] \tag{41}$$

where K_{la} is the scale factor converting horizontal distances to display angles, in the approach display mode.

32

The display coordinates of the longitudinal position indicator (X_s, Y_s) are given by the equations

$$X_s = X_f + 1.25$$
$$Y_s = Y_f + f_s \tag{42}$$

Acceleration Error Ribbon (A)

The acceleration error ribbon (fig. 19) is used only for decelerating approaches to a hover. This symbol is designed to provide longitudinal deceleration guidance to enable the pilot to bring the aircraft to a low speed in the vicinity of the initial station-keeping point. At a predetermined low speed (V_{vl} = 35 ft/s) relative to the initial station-keeping point, the acceleration error ribbon disappears, and, simultaneously, the velocity error line appears. The final transition task of acquiring the station-keeping point is performed using the velocity error line and the longitudinal position indicator (fig. 19). The switch in the longitudinal guidance symbology occurs when the aircraft is about 400 ft from the station-keeping point.

The length of the acceleration error ribbon, f_{ae}, is proportional to the difference between the acceleration along the track, $\widehat{v}_{rt}$, suitably filtered, and a reference acceleration, $\dot{v}_r$, thus

$$f_{ae} = \begin{cases} K_{ax}(\widehat{\dot{v}}_{rt} - \dot{v}_r) & \text{if } v_{rt} \geq V_{vl} \\ 0 & \text{if } v_{rt} < V_{vl} \end{cases} \tag{43}$$

The smoothed acceleration, $\widehat{\dot{v}}_{rt}$, is calculated as follows:

$$\widehat{\dot{v}}_{rt} = \begin{cases} \dot{v}_{rt}/(T_5 s + 1) & \text{if } I_a = 0 \\ \\ \dot{v}_{xc}/\cos(\psi - \psi_t) & \text{if } I_a = 1 \end{cases} \tag{44}$$

where

$\quad I_a \qquad$ acceleration command mode indicator
$\quad \dot{v}_{rt} \qquad$ acceleration along the reference flightpath
$\quad \dot{v}_{xc} \qquad$ pilot-commanded longitudinal acceleration

The value of $\dot{v}_{rt}$ is calculated using the equation

$$\dot{v}_{rt} = \dot{v}_n \cos \psi_t + \dot{v}_e \sin \psi_t + (v_e \cos \psi_t - v_n \sin \psi_t)\frac{iv_{rt}}{R} \tag{45}$$

where v_{rt} is the velocity resolved along the reference flightpath, obtained by the equation

$$v_{rt} = v_n \cos \psi_t + v_e \sin \psi_t$$

On straight segments of the reference flightpath, $1/R = 0$ and equation (45) reduces to the first two terms.

The acceleration command mode indicator, I_a, is unity if the aircraft has a longitudinal acceleration command system; otherwise it is zero. When $I_a = 1$, the commanded acceleration, $\dot{v}_{xc}$, is used in preference to aircraft acceleration, because of its noise-free quality. However, since $\dot{v}_{xc}$ is the commanded acceleration along the longitudinal axis of the aircraft, it is necessary to correct it (eq. (44)) for the crosstrack angle of the aircraft relative to the reference flightpath ($\psi - \psi_t$). The appropriate lateral acceleration required to produce a resultant acceleration along the flightpath is automatically supplied by the pilot as he keeps the flightpath symbol coincident with the ghost aircraft symbol.

The reference acceleration, $\dot{v}_r$, which is computed continuously, is that required to bring the aircraft to a hover at the initial station-keeping point, consistent with the particular deceleration technique adopted for the longitudinal guidance. In most of the simulation evaluations of the HUD, a two-step deceleration technique was adopted. The equations for $\dot{v}_r$ appropriate to this type of guidance are given in appendix C.

The display coordinates of the center of the free end of the acceleration error ribbon (X_{ae}, Y_{ae}) are given by the equations

$$X_{ae} = X_f + 1.09$$

$$Y_{ae} = Y_f + f_{ae}$$

Lateral Acceleration Ball (A)

The distance, f_{ay}, of the lateral acceleration ball from the vertical marker atop the flightpath symbol (fig. 19) is proportional to the body-axis lateral acceleration at the cockpit, a_{yp}, thus

$$f_{ay} = -K_{ay} \left(\frac{a_{yp}}{g} \right)$$

where K_{ay} is the scale factor converting lateral acceleration, in 'g' units, to display angles, in degrees. Since the maximum deflection of the ball on the display is $\pm 1°$, it follows that the full scale deflection of the acceleration ball is equivalent to $\pm 1/K_{ay}$, in 'g' units.

The display graphics are designed to move the acceleration ball across the top of the flightpath symbol, with the position of the ball uniquely specified by the value of f_{ay}.

34

Runway and Landing-Pad Symbols (A,H)

The runway and landing-pad symbols are conformal outlines of the real runway and landing pad. The equations to be presented are general for a landing pad of arbitrary polygonal shape, and therefore also apply to the runway as a special case. The equations are adaptable to most commonly used landing pads, such as heliports, oil rig platforms and ships. The landing pad illustrated in figure 20 consists of two perpendicular rectangles, and has been used in past simulations to represent the landing deck and hangar wall of a destroyer.
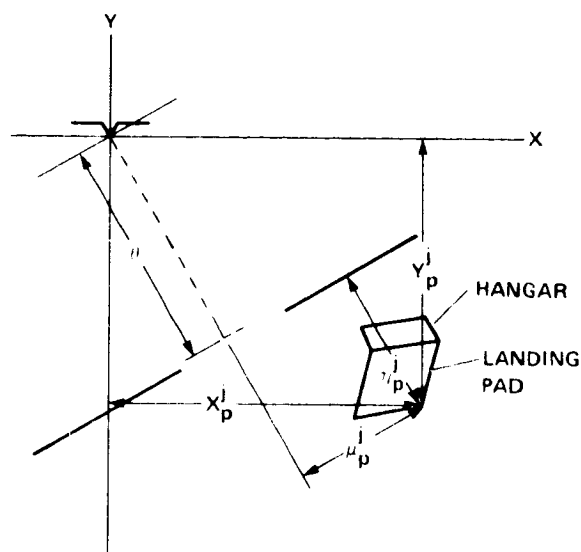
Figure 20.– Geometry of displayed landing-pad position.

If the landing pad has n vertices, then the elevations, η_p^j ($j = 1, n$), of these vertices relative to the horizontal, and their azimuths, μ_p^j ($j = 1, n$), relative to the aircraft's heading, are given (fig. 21) by

$$\eta_p^j = \frac{180}{\pi} \arctan\left(\frac{z_p'' - \delta z''^j}{d_p^j}\right) \quad j = 1, n \tag{46}$$

$$\mu_p^j = \frac{180}{\pi} \arctan\left(\frac{\delta y''^j - y_p''}{\delta x''^j - x_p''}\right) \quad j = 1, n \tag{47}$$

where

$$d_p^j = \sqrt{(\delta x''^j - x_p'')^2 + (\delta y''^j - y_p'')^2} \quad j = 1, n \tag{48}$$

35

and where

x_p'', y_p'', z_p'' coordinates of the pilot's eyepoint relative to the
landing-pad datum, in a local horizontal coordinate
system generated by rotating the standard north-east-down
system about the vertical, through the aircraft's heading angle

$\delta x''^j, \delta y''^j, \delta z''^j$ coordinates of the jth landing-pad vertex in the above
local horizontal coordinate system
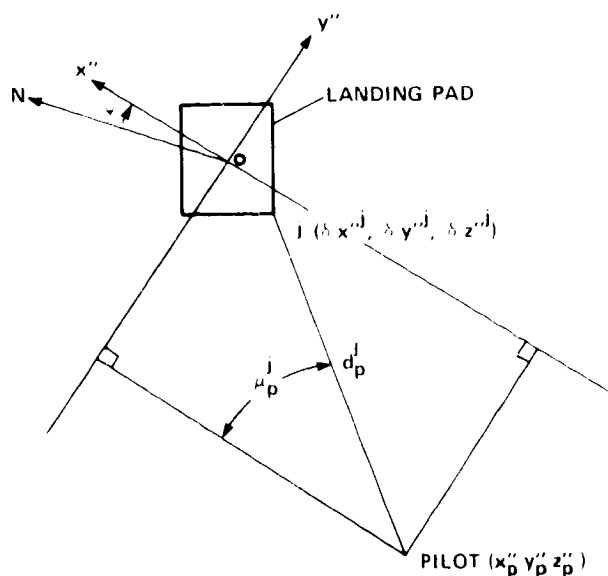
Figure 21.– Horizontal situation geometry.

The coordinates $(\delta x''^j, \delta y''^j, \delta z''^j)$ are obtained from the coordinates $(\Delta x^j, \Delta y^j, \Delta z^j)$ of the vertices in a landing-pad fixed-axis system, by standard Euler-angle transformations.

The positions of the pad vertices in display coordinates (fig. 20) are given by

$$X_p^j = \mu_p^j \cos \phi - (\eta_p^j - \theta) \sin \phi \quad j = 1, n \tag{49}$$

$$Y_p^j = (\eta_p^j - \theta) \cos \phi + \mu_p^j \sin \phi \quad j = 1, n \tag{50}$$

Trident (H)

The aircraft trident symbol is fixed in the display coordinate axis system, at a vertical distance below the aircraft reference symbol equal to the landing attitude, Θ (fig. 22), thus,

36

$$X_t = 0$$
$$Y_t = -\Theta$$

(51)
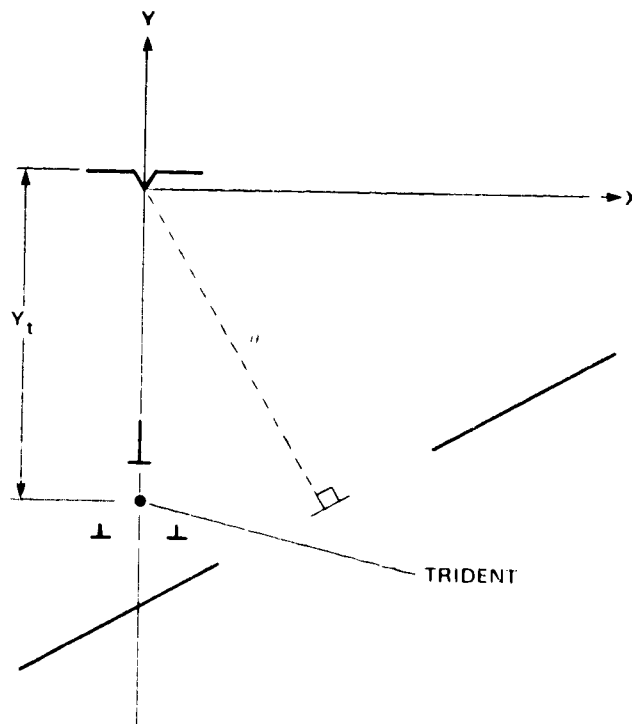
Figure 22.– Display position of aircraft Trident.

Horizontal Velocity Vector (H)

The horizontal velocity vector (fig. 23) is a line, originating at the datum of the aircraft trident symbol, whose length and direction correspond to those of the horizontal velocity vector of the aircraft with respect to the station-keeping point.

The coordinates t_{vx} and t_{vy} of the moving tip of the velocity vector relative to the trident are given by the equations

$$t_{vx} = K_u v_y$$
$$t_{vy} = K_u v_x$$

(52)

where v_x and v_y are the longitudinal and lateral components of the horizontal velocity of the aircraft relative to the landing pad (fig. 15). The equations defining v_x and v_y are

37
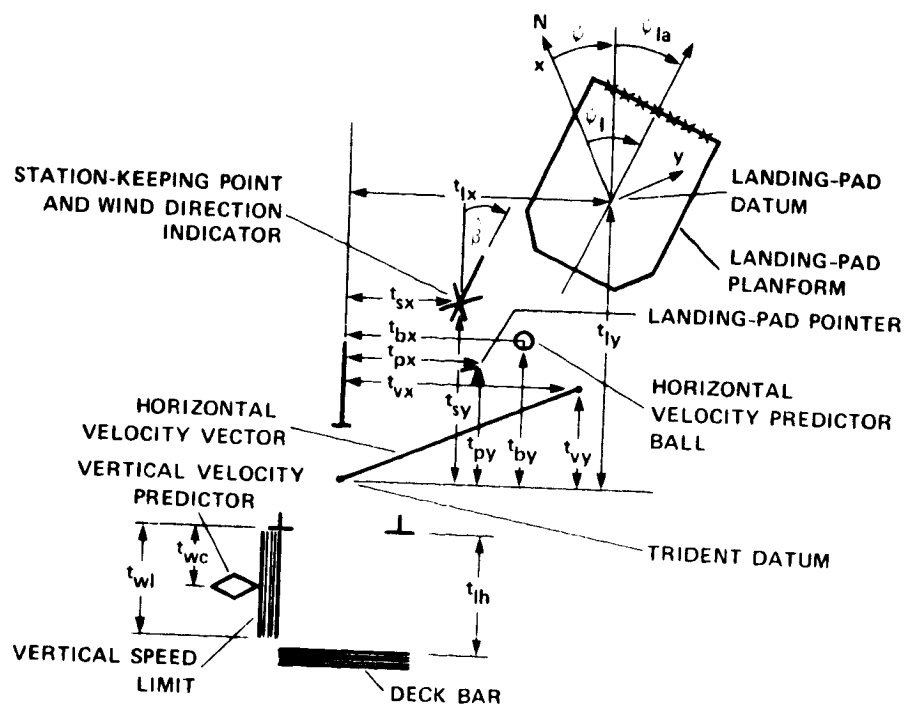
Figure 23.– Position and velocity indicators in hover mode.

$$v_x = v_n \cos \psi + v_e \sin \psi \tag{53}$$

$$v_y = v_e \cos \psi - v_n \sin \psi \tag{54}$$

The display coordinates of the tip of the horizontal velocity vector (X_v, Y_v) are given by the equations

$$X_v = t_{vx}$$
$$Y_v = Y_t + t_{vy} \tag{55}$$

Velocity Predictor Ball (H)

The velocity predictor ball (fig. 23) is used by the pilot to control the horizontal position of the aircraft. The position of this symbol leads that of the tip of the horizontal velocity vector. In the steady state (zero horizontal acceleration), the predictor ball and the tip of the velocity vector coincide.

The laws governing the motion of the predictor ball depend on the type of control system used for low speed and hover. The two classes considered here are identified by I_v, where $I_v = 1$ for

38

translational velocity command and $I_v = 0$ for attitude command. The case $I_v = 0$ includes all control systems that employ only feedback of attitude motion.

The position of the predictor ball (t_{bx}, t_{by}) is proportional to the estimated commanded translational velocities $\widehat{v}_{xc}$ and $\widehat{v}_{yc}$, thus

$$
\begin{aligned}
t_{bx} &= K_u \widehat{v}_{yc} \\
t_{by} &= K_u \widehat{v}_{xc}
\end{aligned}
\tag{56}
$$

If the control system is operating in a translational velocity command mode ($I_v = 1$), then the estimated commanded translational velocities are the true commanded velocities,

$$
\begin{aligned}
\widehat{v}_{xc} &= v_{xc} \\
\widehat{v}_{yc} &= v_{yc}
\end{aligned}
\tag{57}
$$

If the control system employs only feedback of attitude motion ($I_v = 0$) (attitude command, attitude rate command, etc.), then the estimated commanded velocities are obtained by adding, to the aircraft velocities, terms proportional to smoothed estimates of the translational accelerations, $\widehat{v}_x$ and $\widehat{v}_y$, and "washed-out" control inputs. If the control mode is attitude rate command or attitude acceleration command ($I_{at} = 0$) then

$$
\begin{aligned}
\widehat{v}_{xc} &= v_x + T_v \widehat{v}_x - \frac{K_{\delta_x} T_2 s \delta_x}{T_2 s + 1} \\
\widehat{v}_{yc} &= v_y + T_v \widehat{v}_y + \frac{K_{\delta_y} T_2 s \delta_y}{T_2 s + 1}
\end{aligned}
\tag{58}
$$

where

δ_x, δ_y	pilot's control inputs
$K_{\delta_x}, K_{\delta_y}$	control input gains
T_2	control input washout time constant
T_v	horizontal tracking time constant

If the control mode is attitude command or rate command with attitude hold ($I_{at} = 1$), then the input variables δ_x and δ_y in equation (58) are replaced by the commanded pitch and roll angles, θ_c and ϕ_c; also, the gains K_{δ_x} and K_{δ_y} are replaced by gains K_{θ_c} and K_{ϕ_c}. In addition, the value of T_v (table 1) depends on the type of control mode, indicated by I_{at}.

Filtered estimates of the translational accelerations, $\widehat{v}_x$ and $\widehat{v}_y$, are obtained by complementary filtering of the measured attitudes and translational accelerations, thus

39

$$\widehat{\dot{v}}_x = \frac{1}{T_6 s + 1} \left[\frac{-\pi g T_6 s(\dot{\theta} + \dot{\theta}_j)}{180(s + \sigma_u)} + \dot{v}_x \right]$$

$$\widehat{\dot{v}}_y = \frac{1}{T_6 s + 1} \left[\frac{\pi g T_6 s \dot{\phi}}{180(s + \sigma_v)} + \dot{v}_y \right] \tag{59}$$

where

$\dot{v}_x, \dot{v}_y$	longitudinal and lateral accelerations
$\dot{\theta}_j$	engine nozzle angle rate
T_6	complementary filter time constant
σ_u, σ_v	damping parameters for longitudinal and lateral translations

The longitudinal acceleration, $\dot{v}_x$, is given by equation (35). The corresponding equation for the lateral acceleration, $\dot{v}_y$, is

$$\dot{v}_y = \dot{v}_e \cos \psi - \dot{v}_n \sin \psi - (v_n \cos \psi + v_e \sin \psi) \frac{\dot{\psi} \pi}{180} \tag{60}$$

The lateral damping parameter, σ_v, is given by equation (16). The corresponding equation for the longitudinal damping parameter, σ_u, is

$$\sigma_u = \Sigma_u + \Sigma_u' v_{af} \tag{61}$$

where

Σ_u	estimated longitudinal damping parameter in hover ($v_{af} = 0$)
Σ_u'	estimated average rate of change of the longitudinal damping parameter, with airspeed, over the approach airspeed range

The display coordinates of the velocity predictor ball (X_b, Y_b) are given by the equations

$$X_b = t_{bx}$$

$$Y_b = Y_t + t_{by}$$

Landing-Pad Planform (H)

The coordinates (t_{lx}, t_{ly}) of the datum of the landing-pad planform symbol, relative to the trident datum, are derived from those of the aircraft's c.g. relative to the landing pad (x_a, y_a), suitably scaled. The coordinates (x_a, y_a) are relative to a north-east-down coordinate axis system whose origin is at the datum of the landing pad. Since t_{lx} and t_{ly} are relative to the aircraft fixed coordinate system, it is necessary to perform a rotation of the (x_a, y_a) coordinate system about the "down" axis through the aircraft's yaw angle, ψ. The final result is

40

$$t_{lx} = -K_l(y_a \cos \psi - x_a \sin \psi)$$
$$t_{ly} = -K_l(x_a \cos \psi + y_a \sin \psi) \qquad (62)$$

The heading of the landing pad relative to the aircraft's longitudinal axis, ψ_{la}, (fig. 23) is given by

$$\psi_{la} = \psi_l - \psi \qquad (63)$$

The display coordinates of the landing-pad symbol (X_l, Y_l) are given by the equations

$$X_l = t_{lx}$$
$$Y_l = Y_t + t_{ly} \qquad (64)$$

Station-Keeping Point Cross (H)

The location of the station-keeping point cross relative to the trident datum (fig. 23) represents the location of the station-keeping point relative to the aircraft's c.g., scaled to match the sizes of both the aircraft and the landing pad. The initial station-keeping point is located at a fixed position relative to the mean position and orientation of the landing pad. The coordinates t_{sx} and t_{sy} of the initial station-keeping point cross relative to the trident are given by

$$t_{sx} = -K_l[d \sin(\psi - \psi_t) + \delta y \cos(\psi - \psi_t)]$$
$$t_{sy} = K_l[d \cos(\psi - \psi_t) - \delta y \sin(\psi - \psi_t)] \qquad (65)$$

where K_l is the scale factor converting horizontal distances to display angles in the hover display mode.

The final station-keeping point is located at the desired touchdown point, assumed to be the datum of the landing pad. This point therefore moves as the landing pad moves. The coordinates t_{sx} and t_{sy} of the final station-keeping point cross relative to the trident are given by

$$t_{sx} = t_{lx}$$
$$t_{sy} = t_{ly} \qquad (66)$$

The angle $\widehat{\beta}$ of the wind indicator attached to the station-keeping point cross, relative to the aircraft's (trident's) longitudinal axis, is determined by

$$\widehat{\beta} = \psi_{wod} - \psi \qquad (67)$$

41

where ψ_{wod} is the angle of the WOD relative to the longitudinal axis of the landing pad, measured at the landing pad.

The display coordinates of the station-keeping point cross (X_{sc}, Y_{sc}) are given by the equations

$$
\begin{aligned}
X_{sc} &= t_{sy} \\
Y_{sc} &= Y_t + t_{sx}
\end{aligned}
\tag{68}
$$

Station-Keeping Point Pointer (H)

The station-keeping point pointer (fig. 23) is used to indicate the direction of the landing pad when the aircraft is too far away (greater than 136 ft) for the station-keeping point cross to be on the display. The pointer moves in a circle centered on the trident datum.

The coordinates of the station-keeping point pointer (t_{px}, t_{py}) are given by the equations

$$
\begin{aligned}
t_{px} &= R_p \cos \psi_{pa} \\
t_{py} &= R_p \sin \psi_{pa}
\end{aligned}
\tag{69}
$$

where R_p is the radius of the circle on which the pointer moves, and

$$
\psi_{pa} = \frac{180}{\pi} \arctan \left(\frac{t_{sy}}{t_{sx}} \right)
\tag{70}
$$

The display coordinates of the station-keeping point pointer (X_{sp}, Y_{sp}) are given by the equations

$$
\begin{aligned}
X_{sp} &= t_{px} \\
Y_{sp} &= Y_t + t_{py}
\end{aligned}
$$

Landing-Pad Bar (H)

The distance of the landing-pad bar from the base of the trident (t_{lh} in fig. 23) is proportional to the average wheel height above the landing pad. The following equation is used to calculate t_{lh}:

$$
t_{lh} = -K_h(h_t - L_g)
\tag{71}
$$

where

K_h scale factor converting vertical distances to display angles

h_t height of aircraft's c.g. above the reference touchdown point

L_g average distance of the wheels below the aircraft's c.g.

The display coordinates of the center of the upper edge of the landing-pad bar (X_{lh}, Y_{lh}) are given by the equations

$$X_{lh} = 0$$
$$Y_{lh} = Y_t + t_{lh} - 0.5 \tag{72}$$

Vertical Velocity Predictor (H)

The vertical velocity predictor (fig. 23) aids height control in much the same way that the velocity predictor ball aids horizontal position control. The predictor diamond moves vertically relative to the left base of the trident, such that its displacement provides the pilot with an estimate of the commanded vertical velocity, $\widehat{\dot{h}}_c$. The displacement of the diamond, t_{wc}, is given by

$$t_{wc} = K_w \widehat{\dot{h}}_c \tag{73}$$

If the control system is operating in a vertical velocity command mode ($I_w = 1$) then $\widehat{\dot{h}}_c$ is given by equation (10), repeated here for convenience:

$$\widehat{\dot{h}}_c = \dot{h} + \frac{s \dot{h}_c}{s + \Sigma_{wc}} \qquad \text{if } I_w = 1 \tag{10}$$

If vertical control is achieved directly through the engine throttle ($I_w = 0$), with or without a height damper, then one possibility for $\widehat{\dot{h}}_c$ is given by equation (11), which is used for the approach. However, in hover, the vertical acceleration measurement $\ddot{h}$ is less noisy than in the approach, and a better estimate can be obtained from the equation

$$\widehat{\dot{h}}_c = \dot{h} + T_h \widehat{\ddot{h}} \qquad \text{if } I_w = 0 \tag{74}$$

where T_h is the time constant selected for the desired vertical velocity response, and the smoothed vertical acceleration $\widehat{\ddot{h}}$ is obtained by complementary filtering of $\ddot{h}$ and the throttle input δ_t:

$$\widehat{h} = \frac{1}{T_6 s + 1}\left[\ddot{h} + \frac{K_{\delta_t} T_6 s^2 \delta_t}{(s + \sigma_w)}\right] \tag{75}$$

The display coordinates of the center of the vertical velocity predictor diamond (X_w, Y_w) are given by the equations

$$X_w = -1.6025$$
$$Y_w = Y_t + t_{wc} - 0.5 \tag{76}$$

Vertical Velocity Limit Ribbon (H)

The vertical velocity limit ribbon (fig. 23) continuously indicates the maximum acceptable vertical velocity at touchdown. In operation, during the final moments of vertical descent, the pilot maintains the vertical velocity predictor diamond within the span of the vertical velocity limit ribbon, t_{wl}. The equation for t_{wl} is

$$t_{wl} = K_w(\dot{h}_l + \dot{H}) \tag{77}$$

where

$\dot{H}$ recommended maximum touchdown vertical velocity (positive upward)

$\dot{h}_l$ vertical velocity of the landing pad at the touchdown point

The display coordinates of the free end of the vertical velocity limit ribbon (X_{wl}, Y_{wl}) are given by the equations

$$X_{wl} = -0.685$$
$$Y_{wl} = Y_t + t_{wl} - 0.5 \tag{78}$$

CONCLUDING REMARKS

Although the display format described here goes an appreciable way toward meeting the requirements postulated in the section entitled HUD Characteristics, it does not satisfy all of them. Of particular note is the fact that in the approach mode, the flightpath symbol gives the true direction of vertical flight only. Because of HUD field-of-view restrictions, lateral motion of the flightpath symbol has had to be reduced to only 30% ($K_t = 0.3$) of its full value. This scale reduction, coupled with the fact that the yaw scale is conformal, gives the pilot an inaccurate impression of the lateral motion of the aircraft. No difficulties due to the lack of conformality of the flightpath

44

symbol have been encountered in simulation, and moreover, it passed without comment from those who were not informed about it. This may be because the simulator visual attachment, although it has four windows and is wide angle, lacked texture, and may not have provided cues about the direction of flight that were comparable to those provided by the real world. This conjecture will be tested when the display is flown on the NASA V/STOL Research Aircraft. Currently there seems to be no solution to this design problem other than the obvious one of increasing the lateral field of view of the HUD equipment, although a large lateral field of view would almost certainly change the HUD topology from that shown in figure 1.

It should be noted that the described HUD format employs neither color nor occultation. This is because the equipment used did not permit such techniques. It is known from past studies (ref. 8) that color is beneficial in differentiating and highlighting the various symbols, and that it can alleviate the feeling of being overwhelmed by a profusion of symbols. The authors are unaware of any HUD format work in which occultation is being used, although this technique could help by producing an illusion of depth and emphasizing a symbol hierarchy. It is only relatively recently that equipment has become available that permits the use of color and occultation. There is a need for research in these areas.

Another issue that is both important and controversial is the mixing of vertical and horizontal situation information. Admittedly, the result of such mixing is aesthetically unsatisfactory, since not only are the horizontal situation symbols nonconformal, but the pilot is forced to change his or her mental frame of reference between approach and hover. Failure to do the latter can result in confusion, which can cause control reversals, disorientation, and possibly airsickness. An attempt has been made to use vertical situation information and associated guidance in hover (ref. 5), but the result was unsatisfactory. The prime difficulty with the use of vertical situation information is that of representing distances and speeds—particularly closure rates—in a manner that is comparable to the way this information is provided by the real world. The result is a lack of the essential, visually derived lead information needed to perform precise hovering tasks. This could be an important area for future research.

Despite these flaws, the display format appears to meet the requirements of the task for which it was designed. For example, shown in figure 24 are the results of a simulation, performed on the Ames Research Center's VMS, to compare the pilot workload involved in performing shipboard landings using either the simulator visual attachment or the HUD display (but not both). The model of the Spruance-class destroyer described in this report was used, and the sea state varied up to sea state 6 (the precise environment is defined in ref. 8). Two types of control system were tested: one with attitude command, but no control augmentation in the vertical axis, the other with translational velocity command in all three axes. It is clear that, for all the cases tested, the pilot workload was less when the display was used, the reduction being particularly marked (Cooper-Harper handling qualities rating reduction of over 4) in high seas. The workload reduction is largely due to the fact that the display provides the pilot with precise information about the position and velocity of the aircraft relative to the desired touchdown point. This is of particular benefit in the final phase of landing, when the touchdown point is outside the pilot's field of view and its location can only be

45
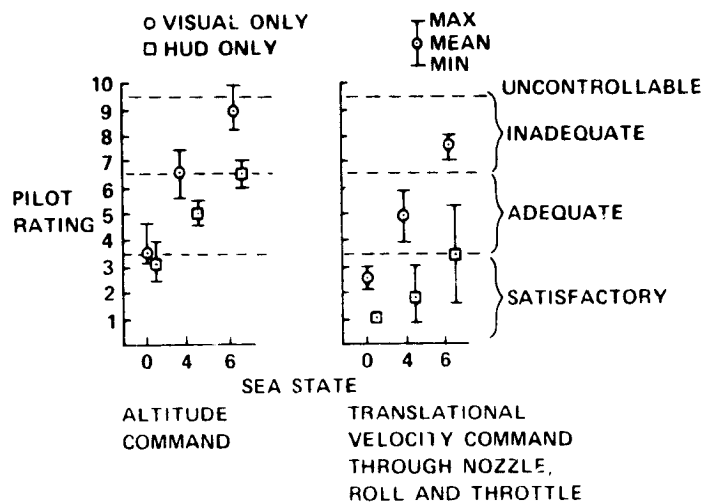
Figure 24.– Pilot ratings for landing.

inferred from the position and orientation of the superstructure—a task that becomes increasingly difficult with increasing sea state.

POSTSCRIPT

Research aimed at further improving the display format and symbol drive laws continues. Some recent contributions are discussed below.

It can be seen from figure 1 that the altitude information is displayed on the left side of the flightpath and trident symbols, and the speed information is displayed on the right. During the latter part of the approach and for hover and vertical landing, the pilot uses a "back side" control technique in which he controls altitude with the left hand (with the throttle or some other advanced controller) and speed with the right hand (with the longitudinal stick or some other advanced controller). Therefore, for the approach and vertical landing, the controls and display are compatible with regard to handedness. In conventional flight, however, most pilots prefer a "front side" control technique, in which altitude is controlled with the right hand and speed with the left. Traditionally, flight instruments have been arranged to be compatible with control handedness in conventional flight, which is, of course, the reverse of that provided by the display described here. Since it is obviously unwise to switch, in flight, the handedness of the displayed information to match whichever control technique is appropriate, and since all pilots are currently trained with the conventional display handedness, the consensus of the pilots currently associated with the display research is that the display should exhibit conventional handedness. To meet this requirement all the symbols that are in fixed positions relative to both the flightpath (fig. 27) and trident (fig. 30) symbols are currently located in positions that are the mirror images of those shown in figures 27 and 30. In addition, the angle-of-attack reference bracket (fig. 28) has been moved to the other side of the flightpath

46

symbol. Pilots have expressed satisfaction with these changes and have adapted to them rapidly, which is remarkable since they had many hours of experience with the display in its previous form.

The original tests used to develop the display format concentrated largely on the more advanced control systems, particularly those with attitude command. With a good attitude command system, the attitude of the aircraft is virtually unaffected by power changes, thrust deflection, and external disturbances. It follows that the pilot's need for attitude awareness is minimized, which allows more time to concentrate on the guidance task. Recently, the display has been used in simulation tests which offered an opportunity to more closely examine its effectiveness in limited-visibility approaches using the basic rate-augmented Harrier control system. It was found that, because this control system does not have the disturbance rejection properties of an attitude command system, the pilots needed to be much more conscious of the aircraft's attitude in order to actively prevent the large deviations that can complicate the guidance task. To help increase this attitude awareness, the aircraft reference symbol has been increased to three times the size shown in figures 25 and 26, so that it now spans 6° and is correspondingly thicker and bolder. This modification was an improvement, but is probably not the final answer to the problem.

REFERENCES

1. Bray, R. S.: A Head-Up Display Format for Application to Transport Aircraft Approach and Landing. NASA TM-81190, 1980.

2. Hynes, C. S.; Franklin, J. A.; Hardy, G. H.; Martin, J. L.; and Innis, R. C.: Flight Evaluation of Pursuit Displays for Precision Approach of Powered-Lift Aircraft. AIAA Journal of Guidance, Control and Dynamics, vol. 12, no. 4, July-Aug. 1989.

3. Merrick, V. K.; and Gerdes, R. M.: VTOL Controls for Shipboard Operations. SAE Aerospace Congress and Exposition Paper 831428, 1983.

4. Merrick, V. K.: Simulation Evaluation of Two VTOL Control/Display Systems in IMC Approach and Landing. NASA TM-85996, 1983.

5. Farris, G. G.; Merrick, V. K.; and Gerdes, R. M.: Simulation Evaluation of Flight Controls and Display Concepts for VTOL Shipboard Operations. AIAA Guidance and Control Conference Paper 2173, 1983.

6. Keane, W. P.; Shupe, N. K.; Robbins, T.; and Campagna, R. W.: A Versatile Display for NOE Operations. 33rd Annual Forum of the AHS, Paper 77.33-24, 1977.

7. Tsoubanos, C. M.: An Investigation of Displayed Ground Referenced Position, Velocity and Acceleration for Precision Hover. ECOM 4334, 1975.

8. Stapleford, R. L.; Clement, W. E.; Booth, G. C.; and Fortenbaugh, R. L.: Flight Control/Flying Qualities Investigation for Lift/Cruise Fan V/STOL. NADC-77143-30, 1979.

APPENDIX A

GEOMETRICAL SPECIFICATIONS

Fixed Geometry Symbols

The displayed information used in the piloted simulation experiments was presented within a total field of view measuring 16° horizontally and 16° vertically. The specifications of those symbols whose geometry is either invariant or simply dependent on aircraft state are given in figures 25 through 31.
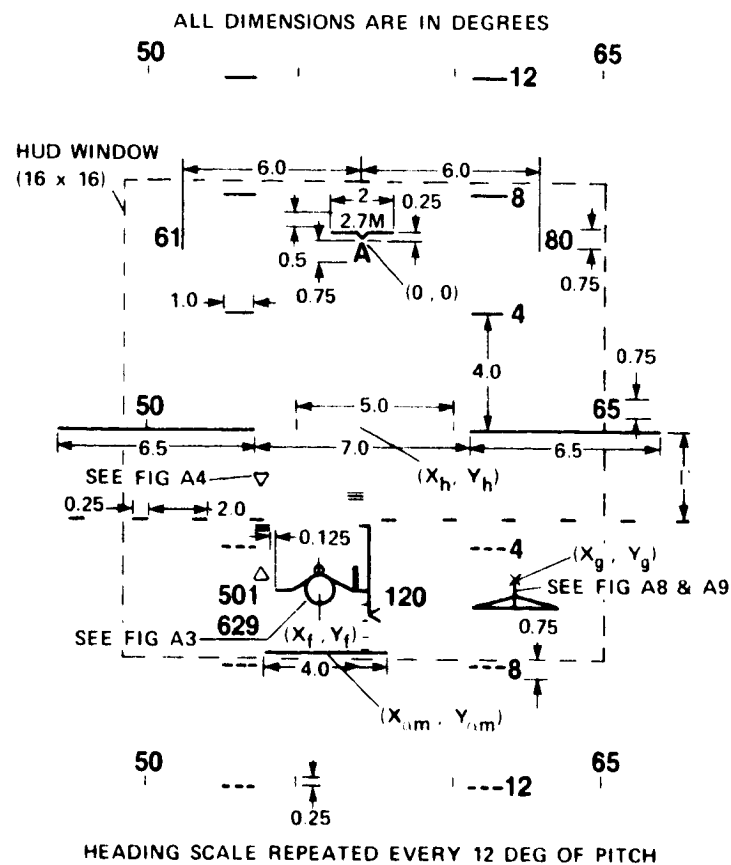
Figure 25.– General arrangement of approach display.
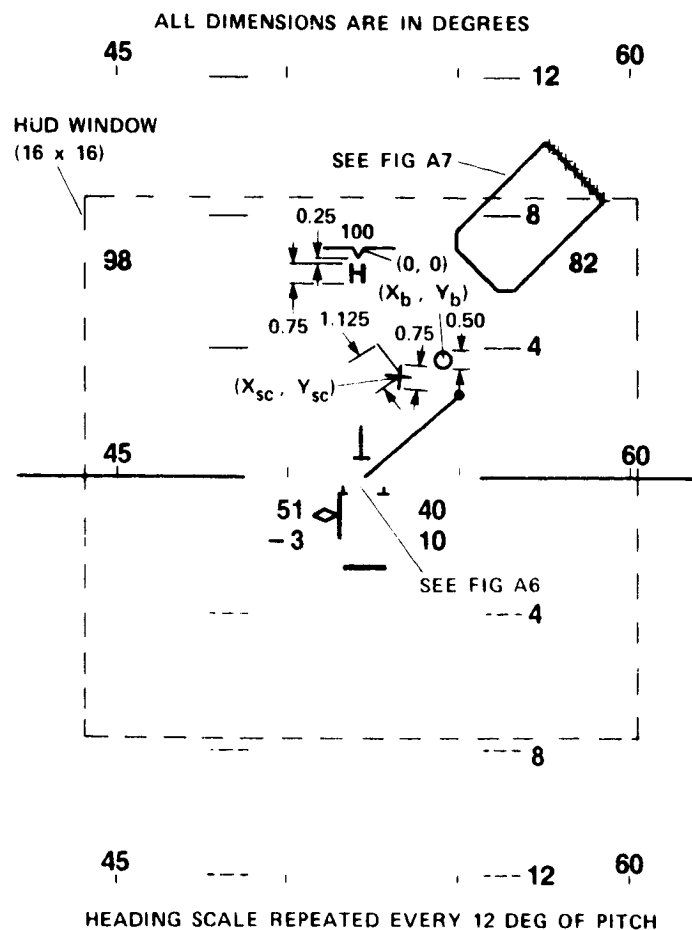
Figure 26.– General arrangement of hover display.

Ghost Aircraft Symbol Geometry

The ghost aircraft symbol (figs. 32, 33) is unique in that its geometrical specification is dependent on aircraft position in a relatively complex way.

The ghost aircraft is a perspective outline drawing of a delta dart configuration, including a vertical fin. The longitudinal axis of the ghost is always tangential to the reference flightpath at the aircraft's location. If the aircraft is exactly on the reference flightpath, the pilot's view of the ghost is that of an inverted 'T' (fig. 8) with a flashing beacon at the tip of the fin. If the aircraft is laterally displaced from the reference flightpath, the pilot sees a projection of the fin. If the aircraft is displaced vertically from the reference flightpath, the pilot sees a projection of the wing. It follows that the appearance of the ghost provides the pilot with status information on the position of the aircraft with respect to the flightpath.

Ghost Aircraft Symbol Equations: The elevation and azimuth deviations (η'_g, μ'_g) of the ghost aircraft symbol caused by aircraft position errors relative to the reference trajectory are given by

50
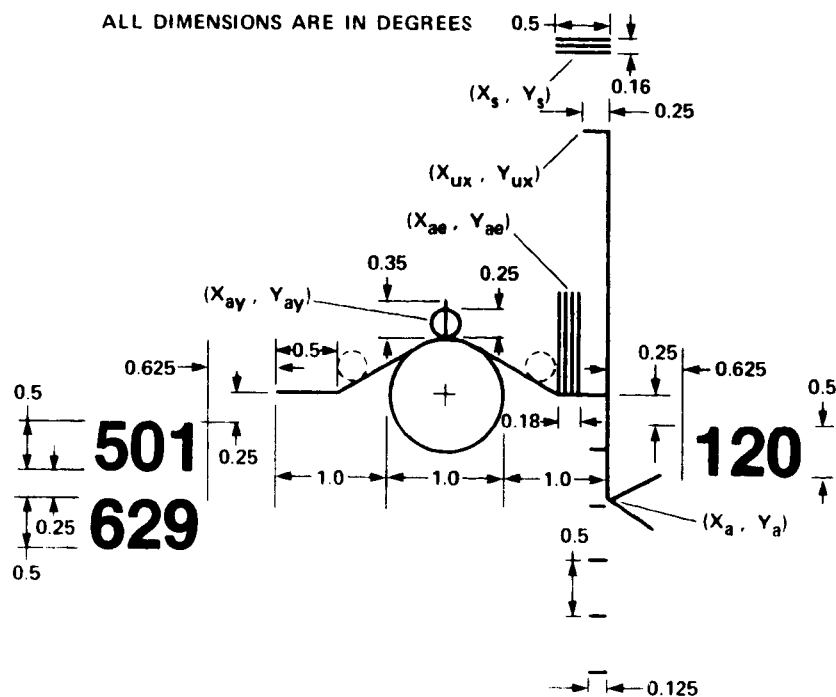
Figure 27.– Flightpath symbol group.

$$\eta'_g = \frac{180}{\pi} \left(\frac{h_r - h}{\delta x_{gh}} \right) \tag{A1}$$

$$\mu'_g = \frac{-180}{\pi} \left(\frac{\delta y}{\delta x_{gy}} \right) \tag{A2}$$

where h_r is the altitude of the reference flightpath at the location of the aircraft, given by

$$h_r = H + d \tan \Gamma \tag{A3}$$

The elevation and azimuth of the defining vertices b, c, d, e, f, and g of the ghost aircraft (fig. 32), relative to the ghost beacon (vertex a), are given by

$$\delta\eta'_{gb} = -\Delta\eta \tag{A4}$$

$$\delta\mu'_{gb} = 0 \tag{A5}$$

$$\delta\eta'_{gc} = -\eta'_g \left(\frac{\pi \Delta \chi}{180 + \pi \Delta \chi} \right) - \Delta\eta \tag{A6}$$

Figure 28.– Angle-of-attack reference bracket.

$$\delta\mu'_{gc} = -\mu'_g \left(\frac{\pi\Delta\chi}{180 + \pi\Delta\chi} \right) \qquad (A7)$$

$$\delta\eta'_{gd} = -\Delta\eta \qquad (A8)$$

$$\delta\mu'_{gd} = -\Delta\mu \qquad (A9)$$

$$\delta\eta'_{ge} = \Delta\eta \qquad (A10)$$

$$\delta\mu'_{ge} = \Delta\mu \qquad (A11)$$

$$\delta\eta'_{gf} = -\Delta\eta \qquad (A12)$$

$$\delta\mu'_{gf} = -\Delta\eta \left(\frac{\delta\mu'_{gc}}{\delta\eta'_{gc}} \right) \qquad (A13)$$

ALL DIMENSIONS ARE IN FEET

RUNWAY

	SUPERSCRIPT j			
	1	2	3	4
Δx^j	0	1500	1500	0
Δy^j	-50	-50	50	50
Δz^j	0	0	0	0
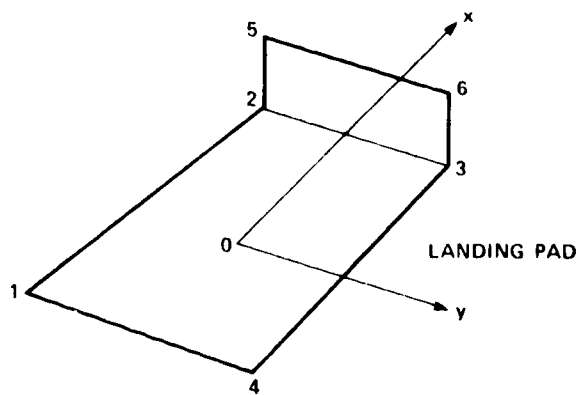
LANDING PAD

	SUPERSCRIPT j					
	1	2	3	4	5	6
Δx^j	-27.5	42.5	42.5	-27.5	42.5	42.5
Δy^j	-20.0	-20.0	20.0	20.0	-20.0	20.0
Δz^j	0	0	0	0	-20.0	-20.0

Figure 29.– Runway and landing-pad geometry (approach mode).

$$\delta \eta'_{gg} = \Delta \mu \left(\frac{\Delta \eta'_{gc} - \Delta \eta}{\Delta \mu + |\delta \mu'_{gc}|} \right) - \Delta \eta \qquad (A14)$$

$$\delta \mu'_{gg} = 0 \qquad (A15)$$

53

Figure 30.– Trident symbol group.

where $\Delta\eta$, $\Delta\mu$, and $\Delta\chi$ are the dimensions of the vertical fin, wing semispan, and length of the ghost aircraft in display angles (fig. 32).

The conditions for the existence of the various lines comprising the ghost are (fig. 33)

$$\overline{bc} \qquad \text{if } \eta'_g < 0$$
$$\overline{ac} \qquad \text{if } \eta'_g < 0 \quad \text{or } |\delta\mu'_{gf}| > \Delta\mu$$
$$\overline{af} \qquad \text{if not } \overline{ac}$$
$$\overline{dc} \qquad \text{if } \mu'_g > 0 \quad \text{or } \eta'_g > 0 \quad \text{or } \delta'_{gg} > 0$$
$$\overline{dg} \qquad \text{if not } \overline{dc}$$
$$\overline{ec} \qquad \text{if } \mu'_g < 0 \quad \text{or } \eta'_g > 0 \quad \text{or } \delta\eta'_{gg} > 0$$
$$\overline{eg} \qquad \text{if not } \overline{ec}$$

The display coordinates of the defining vertices of the ghost aircraft symbol $(X_{g-}, Y_{g-}$ where $- = b, c, d, e, f, g)$ are given by

$$X_{g-} = X_g + \delta\mu'_{g-} \cos\delta\phi_g + \delta\eta'_{g-} \sin\delta\phi_g \qquad (A16)$$
$$Y_{g-} = Y_g + \delta\eta'_{g-} \cos\delta\phi_g - \delta\mu'_{g-} \sin\delta\phi_g \qquad (A17)$$

where the roll angle, $\delta\phi_g$, of the ghost relative to the aircraft is given by equation (28) and the display coordinates (X_g, Y_g) of the ghost beacon (vertex a) are given by equation (26).

54

ALL DIMENSIONS ARE IN DEGREES
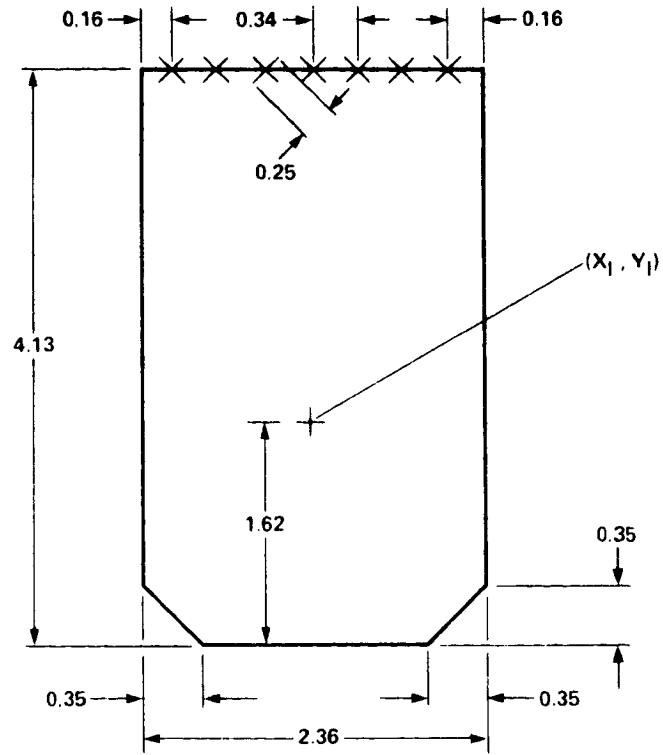
LANDING PAD BASED ON THAT OF A DD 963

Figure 31.– Landing pad details (hover mode).
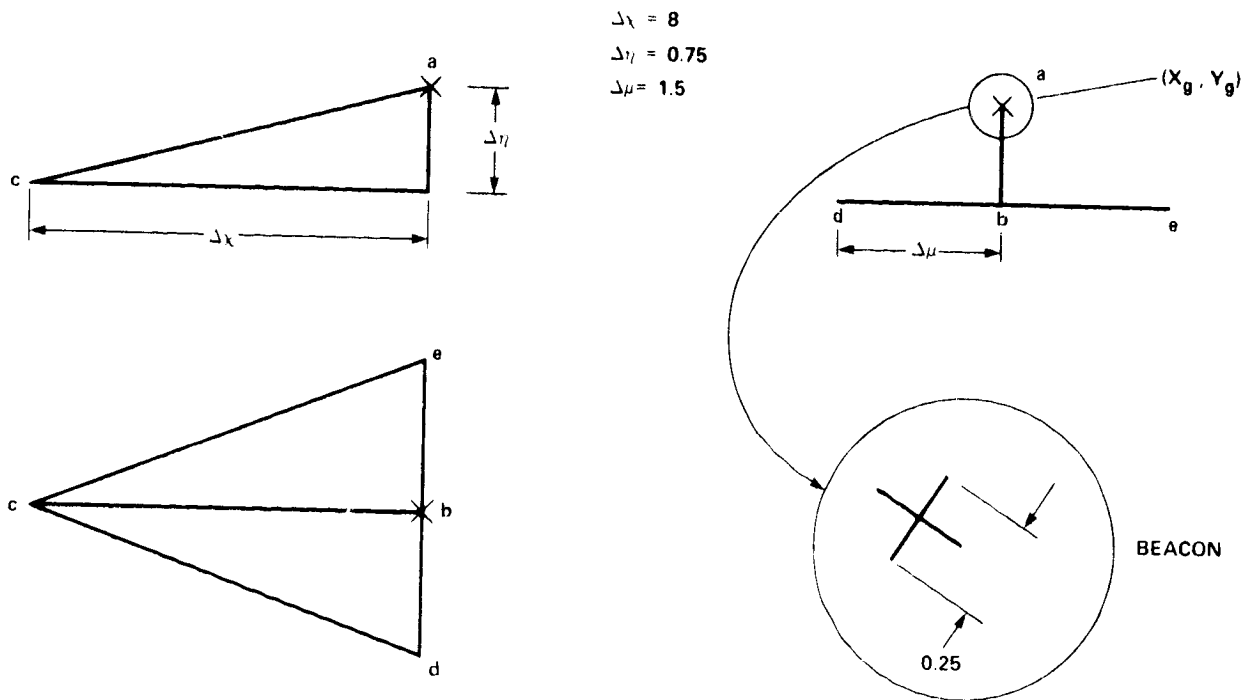
Figure 32.– Ghost aircraft geometry.
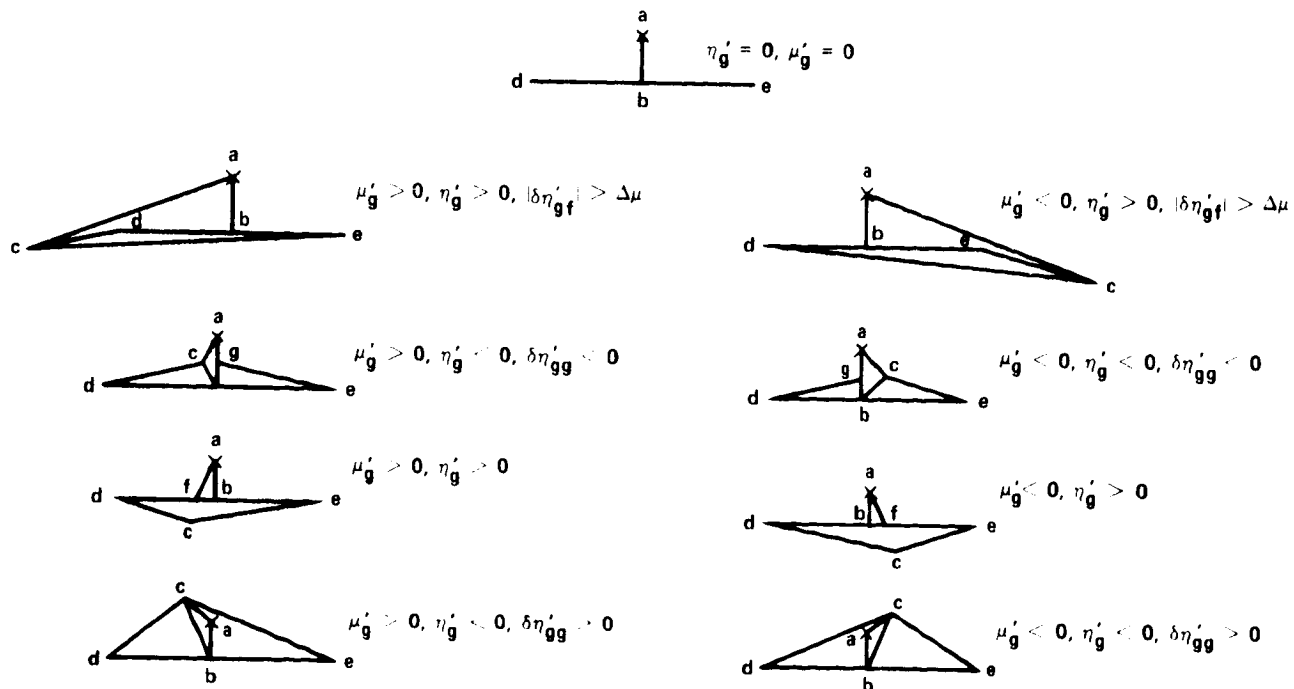
Figure 33.– Possible views of ghost aircraft.

APPENDIX B

FLIGHTPATH SYNTHESIS

Preliminaries

It is assumed that the onboard navigation sensors provide sufficient information and that there is sufficient processing capability to permit onboard continuous synthesis of a reference flightpath that is a member of a predefined class of flightpaths. When the synthesized flightpath is acceptable to the pilot, he selects it by "freezing" the synthesizing process.

The class of approach flightpaths used in conjunction with the HUD is illustrated in figure 34. The heading, Ψ_f, and length, D_c, of the final straight segment of the flightpath, along with the radius, R, of the two circles, are preset by the pilot. From any aircraft position, the instantaneous reference flightpath is defined as the line tangential to one of the circles and passing through the aircraft, followed by a segment of the circle and finally by the preset straight-line segment. The flightpath ends either at touchdown or at the station-keeping point. The horizontal plane is divided into two parts by a line coincident with the final straight segment. This division determines which of the two circles will be used. If the aircraft flies across the boundary during the process of continuous flightpath synthesis, the first segment of the flightpath moves from being tangential to one circle to being tangential to the other. If the aircraft passes within either of the circles before the pilot selects a flightpath, the first segment switches from the circle entered to the other circle (fig. 34).
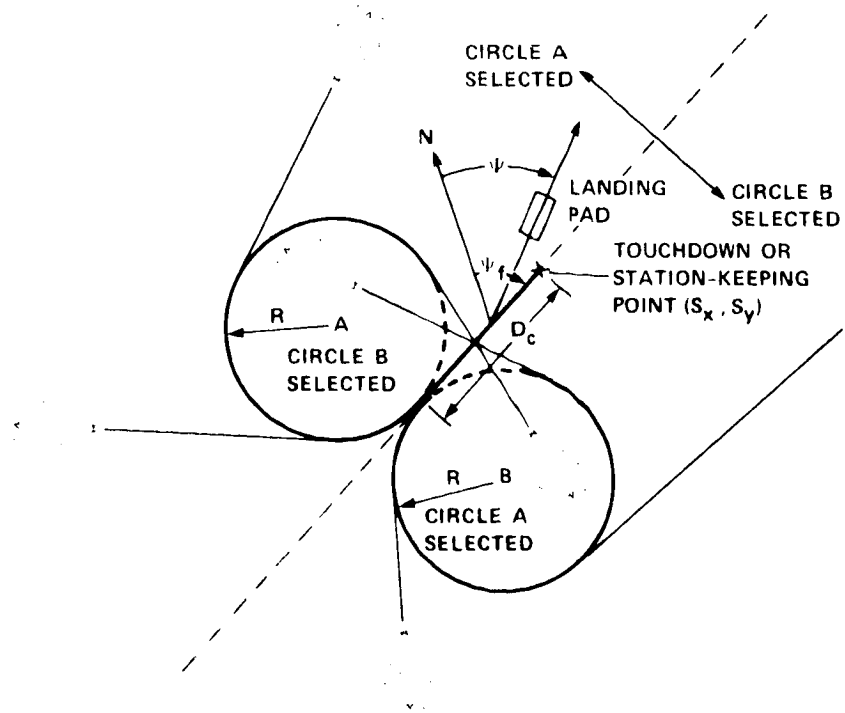
Figure 34.– Class of reference flightpaths.

57

Required Data

The following information must be provided to the system:

S_x, S_y touchdown or station-keeping point coordinates in the landing-pad reference frame

Ψ landing-pad heading ($0 \leq \Psi < 360$)

Ψ_f heading of the final flightpath segment ($0 \leq \Psi_f < 360$)

D_c length of the final flightpath segment

R radius of the circular flightpath segments

These parameters are generally constant, but they may be changed up to the time the pilot selects the reference flightpath. After the reference flightpath has been selected, no further changes in these parameters can be made. In addition to these parameters, the navigation system must continuously provide the coordinates (x_a, y_a) of the aircraft in the landing-pad reference frame.

Synthesis

From the basic data, the coordinates of the point C (fig. 35) and the centers of the circles can be calculated. The coordinates of point C are given by the equations

$$C_x = S_x - D_c \cos \Delta\Psi_f \qquad (B1)$$

$$C_y = S_y - D_c \sin \Delta\Psi_f \qquad (B2)$$

where $\Delta\Psi_f$ is the heading of the final flightpath segment relative to the x axis of the landing pad, and is given by the equation

$$\Delta\Psi_f = \Psi_f - \Psi \qquad (B3)$$

The coordinates $(R_x^{(i)}, R_y^{(i)})$ of the centers of the circles are given by the equations

$$R_x^{(i)} = C_x - iR \sin \Delta\Psi_f \qquad (B4)$$

$$R_y^{(i)} = C_y + iR \cos \Delta\Psi_f \qquad (B5)$$

where $i = +1$ or $i = -1$ denotes the circle for flight in the clockwise or anticlockwise direction, respectively.

The appropriate circle depends on the distances $l^{(i)}$, $i = +1, -1$, of the aircraft from the centers of the circles, given by
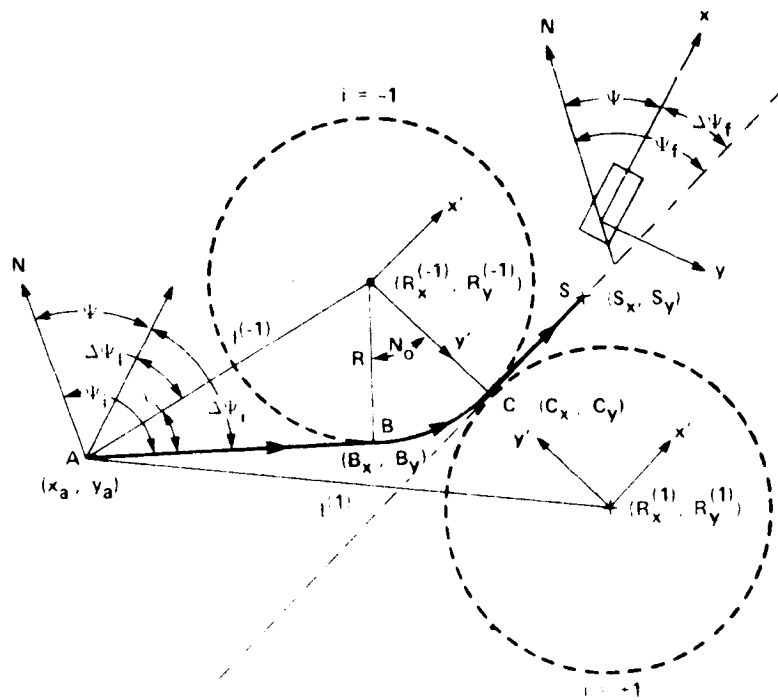
Figure 35.– Flightpath geometry.

$$l^{(i)} = \sqrt{(x_c - R_x^{(i)})^2 + (y_a - R_y^{(i)})^2} \,, \qquad i = +1, -1 \qquad (B6)$$

and the circle selection conditions

$$
\begin{aligned}
&\text{if } l^{(+1)} < R \text{ then } i = -1\\
&\text{if } l^{(-1)} < R \text{ then } i = +1\\
&\text{if } l^{(+1)} \geq R \text{ and } l^{(-1)} \geq R \text{ and } l^{(+1)} > l^{(-1)} \text{ then } i = -1\\
&\text{if } l^{(+1)} \geq R \text{ and } l^{(-1)} \geq R \text{ and } l^{(+1)} \leq l^{(-1)} \text{ then } i = +1
\end{aligned}
$$

Further calculations require knowledge of the angles $\Delta\Psi_l$ and λ. The former angle is that between the line from the aircraft to the center of the appropriate circle (AL or AR of fig. 35) and the x axis of the landing pad. The latter is the angle between AL or AR and the first flightpath segment. These two quantities are calculated from the equations

$$\Delta\Psi_l = \frac{180}{\pi} \arctan\left(\frac{R_y^{(i)} - y_a}{R_x^{(i)} - x_a}\right) \,, \qquad 0 \leq \Delta\Psi_l < 360 \qquad (B7)$$

$$\lambda = \frac{180}{\pi} \arcsin\left(\frac{R}{l^{(i)}}\right) \,, \qquad 0 \leq \lambda \leq 90 \qquad (B8)$$

The track angle of the initial flightpath segment relative to the x axis of the landing pad, $\Delta\Psi_i$, may now be calculated from the equation

$$\Delta\Psi_i = \Delta\Psi_l - i\lambda \qquad (B9)$$

and the initial flightpath heading is given by

$$\Psi_i = \Psi + \Delta\Psi_i, \qquad 0 \leq \Psi_i < 360 \qquad (B10)$$

The coordinates (B_x, B_y) of the point B at the start of the circular segment may now be calculated using the equations

$$B_x = R_x^{(i)} + iR\sin\Delta\Psi_i \qquad (B11)$$

$$B_y = R_y^{(i)} - iR\cos\Delta\Psi_i \qquad (B12)$$

The angle N_0 that the circular segment subtends at the center of the circle is obtained using the equation

$$N_0 = 180(i+1) - i(\Psi_i - \Psi_f), \qquad 0 \leq \Psi_i - \Psi_f < 360 \qquad (B13)$$

The calculation is completed by determining the distances D_b, from point B to point S, and d, from the aircraft to point S (measured along the reference flightpath), thus

$$D_b = D_c + \frac{\pi R N_0}{180} \qquad (B14)$$

$$d = l^{(i)}\cos\lambda + D_b \qquad (B15)$$

The quantities i, Ψ_i, B_x, B_y, d, and D_b are calculated continuously up to the instant that the pilot selects the reference flightpath. Before the selection, $\delta y = 0$. After selection, the quantities i, Ψ_i, B_x, B_y, and D_b (in addition to S_x, S_y, Ψ, Ψ_f, D_c, and R) remain constant at their values at the instant of flightpath selection.

60

APPENDIX C

GUIDANCE

Lateral Guidance

Lateral guidance is provided by the ghost aircraft symbol, and the lateral guidance law is provided by the geometrical relationship between the aircraft and the ghost (fig. 16). To calculate the azimuth angle of the ghost, μ_g, (eq. (23)) and the ghost bank-angle-blend function, k_ϕ, (eq. (29)), requires knowledge of the range, d, the lateral offset of the aircraft from the reference flightpath track, δy, and the heading of the reference flightpath, ψ_t. Which equations are needed to determine these quantities depends on which segment of the reference flightpath the aircraft is located in (fig. 36).
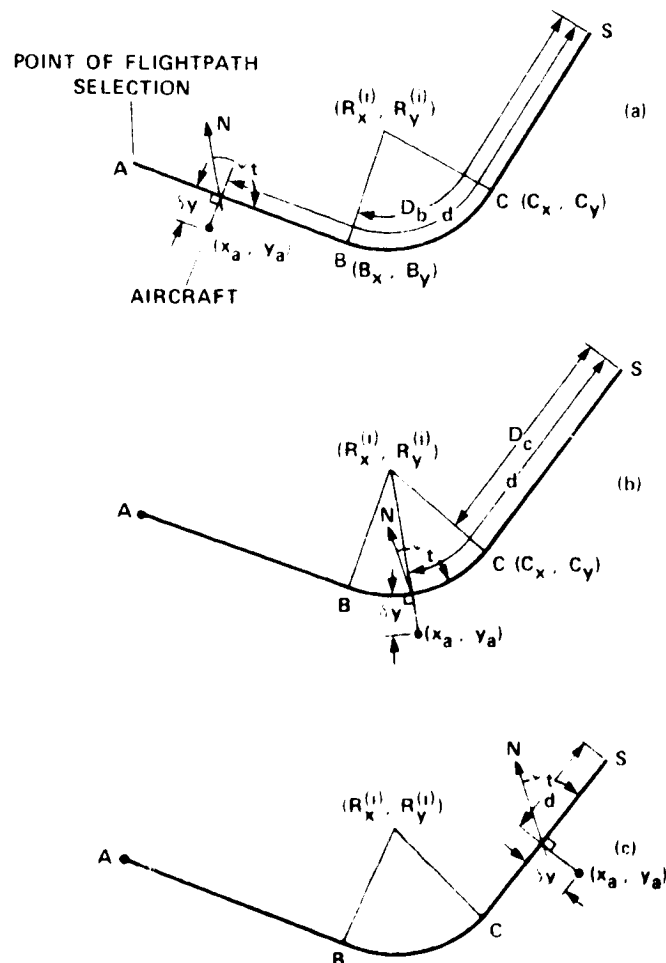
Figure 36.– Illustration of variables d, δy, ψ_t in the three flightpath segments.

Segment AB (fig. 36(a)) $\qquad d > D_b$

$$d = D_b - (x_a - B_x) \cos \Delta\Psi_i - (y_a - B_y) \sin \Delta\Psi_i \qquad (C1)$$

$$\delta y = -(x_a - B_x) \sin \Delta\Psi_i + (y_a - B_y) \cos \Delta\Psi_i \qquad (C2)$$

$$\psi_t = \Psi_i \qquad (C3)$$

Segment BC (fig. 36(b)) $\qquad D_b \geq d > D_c$

$$d = D_c + \frac{\pi R \nu}{180} \qquad (C4)$$

$$\delta y = i(R - l^{(i)}) \qquad (C5)$$

$$\psi_t = \Psi_f - i\nu \qquad (C6)$$

where ν is the angle subtended at the center of the circle by the remaining part of the circular-arc segment. The value of ν is determined by the equation

$$\nu = \frac{180}{\pi} \arctan\left(\frac{-x_a'}{y_a'}\right), \qquad 0 \leq \nu < 360 \qquad (C7)$$

where x_a', y_a' are the coordinates of the aircraft in an axis system (x', y') whose origin is at the center of the appropriate circle and whose x' axis is parallel to the final flightpath segment (fig. 35). The coordinates x_a' and y_a' are calculated from previously determined quantities by the equations

$$x_a' = (x_a - R_x^{(i)}) \cos \Delta\Psi_f + (y_a - R_y^{(i)}) \sin \Delta\Psi_f \qquad (C8)$$

$$y_a' = i[(x_a - R_x^{(i)}) \sin \Delta\Psi_f - (y_a - R_y^{(i)}) \cos \Delta\Psi_f] \qquad (C9)$$

Segment CS (fig. 36(c)) $\qquad D_c \geq d$

$$d = -(x_a - S_x) \cos \Delta\Psi_f - (y_a - S_y) \sin \Delta\Psi_f \qquad (C10)$$

$$\delta y = (y_a - S_y) \cos \Delta\Psi_f - (x_a - S_x) \sin \Delta\Psi_f \qquad (C11)$$

$$\psi_t = \Psi_f \qquad (C12)$$

62

Vertical Guidance

Vertical guidance, like lateral guidance, is provided by the ghost aircraft symbol. In this case the key variable is the altitude of the ghost, h_g, given by equation (21).

Longitudinal Guidance

It is assumed that the deceleration profile should contain flexibility to permit the pilot to select the maximum deceleration. It is also assumed that both the final deceleration and its period should be constant. The latter assumption is motivated by the viewpoint that the kinematics of the critical final approach to the initial station-keeping point should be independent of the aggressiveness of the initial deceleration. A two-step deceleration profile (fig. 37) is compatible with these assumptions.
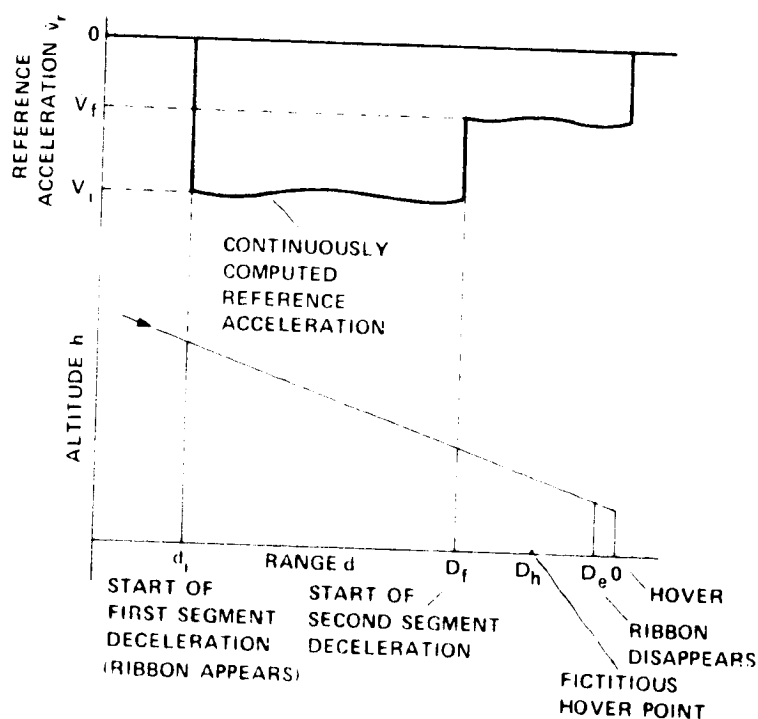
Figure 37.– Two-step deceleration technique.

The selection of the final deceleration and its period rests on pilot judgment of the maximum comfortable closure rate to the station-keeping point, which, in turn, depends on the proximity of solid obstacles to the station-keeping point. When operating to ships, simulation indicates that a final deceleration of 1.5 ft/sec² and period of 35 sec are acceptable. Without obstacles, a higher final deceleration for a reduced period may be acceptable.

Given the nominal final deceleration, $-\dot{V}_f$, and period, ΔT_f, the nominal range, D_f, at the start of the final deceleration is given by

63

$$D_f = \frac{-\dot{V}_f (\Delta T_f)^2}{2} \tag{C13}$$

The pilot selects the value of the nominal initial deceleration, $-\dot{V}_i$. The guidance system then calculates the range, D_h, at which the aircraft would come to a hover if the deceleration were held constant at $-\dot{V}_i$, as follows:

$$D_h = D_f \left(1 - \frac{\dot{V}_f}{\dot{V}_i} \right) \tag{C14}$$

Before the aircraft reaches the start of the deceleration, the guidance system continuously calculates the reference initial deceleration, $-\dot{v}_r$, appropriate to the current position, d, and the speed of the aircraft along the reference trajectory, v_{rt}, from the equation

$$\dot{v}_r = \frac{-v_{rt}^2}{2(d - D_h)} \tag{C15}$$

In addition, a continuous calculation is made to establish the range, d_i, at which the aircraft's acceleration, $\dot{v}_r$, will equal the selected value, $-\dot{V}_i$, where

$$d_i = \frac{v_{rt}^2}{2\dot{V}_i} + D_h \tag{C16}$$

When $d < d_i$, the deceleration error ribbon appears on the display and flashes for 2 seconds at 3 Hz, to prompt the pilot to start the deceleration. The reference deceleration, $-\dot{v}_r$, continues to be calculated using equation (C15) until the range is less than D_f, after which the calculation is switched to

$$\dot{v}_r = \frac{-v_{rt}^2}{2d} \tag{C17}$$

When the longitudinal velocity is less than V_{vl}, the acceleration error ribbon is removed from the display, as described in the section entitled "Acceleration Error Ribbon (A)."

64

Report Documentation Page

1. Report No. NASA TM-102216	2. Government Accession No.	3. Recipient's Catalog No.
4. Title and Subtitle A Head Up Display Format for Application to V/STOL Aircraft Approach and Landing		5. Report Date January 1990
		6. Performing Organization Code
7. Author(s) Vernon K. Merrick, Glenn G. Farris, and Andrejs A. Vanags*		8. Performing Organization Report No. A–89215
		10. Work Unit No. 505-61-71
9. Performing Organization Name and Address Ames Research Center Moffett Field, CA 94035-1000		11. Contract or Grant No.
		13. Type of Report and Period Covered Technical Memorandum
12. Sponsoring Agency Name and Address National Aeronautics and Space Administration Washington, DC 20546-0001		14. Sponsoring Agency Code

15. Supplementary Notes

Point of Contact: Vernon K. Merrick, Ames Research Center, MS 211-2,
                    Moffett Field, CA 94035-1000, (415) 604-6194 or FTS 464-6194

*SYRE Corporation, Moffett Field, CA

16. Abstract

This paper describes, in detail, a head up display (HUD) format developed at NASA Ames Research Center to provide pilots of V/STOL aircraft with complete flight guidance and control information for Category-IIIC terminal-area flight operations. These flight operations cover a large spectrum, from STOL operations on land-based runways to VTOL operations on small ships in high seas. Included in this description is a complete geometrical specification of the HUD elements and their drive laws. The principal features of this display format are the integration of the flightpath and pursuit guidance information into a narrow field of view, easily assimilated by the pilot with a single glance, and the superposition of vertical and horizontal situation information. The display is a derivative of a successful design developed for conventional transport aircraft. The design is the outcome of many piloted simulations conducted over a four-year period. Whereas the concepts on which the display format rests could not be fully exploited because of field-of-view restrictions, and some reservations remain about the acceptability of superimposing vertical and horizontal situation information, the design successfully fulfilled its intended objectives.

17. Key Words (Suggested by Author(s)) Head up display VTOL Shipboard landing		18. Distribution Statement Unclassified-Unlimited Subject Category - 06	
19. Security Classif. (of this report) Unclassified	20. Security Classif. (of this page) Unclassified	21. No. of Pages 77	22. Price A05